Heliyon 10 (2024) e38364

Contents lists available at ScienceDirect

Heliyon

journal homepage: www.cell.com/heliyon

Research article

Hydrogeochemical evolution and heavy metal characterization of groundwater from southwestern, Nigeria: An integrated assessment using spatial, indexical, irrigation, chemometric, and health risk models

Toheeb Lekan Jolaosho [a,*], Adejuwon Ayomide Mustapha [a], Samuel Todeyon Hundeyin [b]

[a] Department of Fisheries, Faculty of Science, Lagos State University, Ojo, Lagos State, Nigeria
[b] Department of Geography and Planning, Lagos State University, Ojo, Lagos State, Nigeria

ARTICLE INFO

Keywords:
Aquifer system
Groundwater quality index
Heavy metal pollution index
Hydrogeochemical processes
Multivariate analysis
Health risk assessment

ABSTRACT

This study examines the hydrogeochemical and heavy metal parameters of groundwater in Ojo District to determine its suitability for use, potential sources, and human health implications. Ten groundwater samples were assessed, and hydrogeochemical modelling was performed via the Aquachem software. The chemical ions were in the following order: EC > (107.78–448.65 μS/cm) > TDS (182.02–320.77 mg/l) > TH (46.22–182.45 mg/l) > pH (5.55–6.35); HCO_3^- (64.13–125.82 mg/l) > Na^+ (36.87–96.49 mg/l) > Ca^{2+} (47.65–58.88 mg/l) > SO_4^{2-} (19.94–53.67) > NO_3^- (15.55–44.25 mg/l) > Cl^- (20.43–27.16 mg/l) > Mg^{2+} (11.09–16.87 mg/l) and K^+ (2.55–7.86 mg/l). The concentrations of heavy metals in groundwater were in the range of: Fe (0.11–0.27 mg/l) > Mn (0.003–0.16 mg/l) > Ni (0.05–0.12 mg/l) > Zn (0.003–0.05 mg/l) > Pb (0.001–0.03 mg/l) > As (0.001–0.005 mg/l) > Cr (0.002–0.005 mg/l) > Cd (0.001–0.003 mg/l) and Cu (0.001–0.0002 mg/l), with Pb, Mn, and Ni exceeding their allowable limits. The Schoeller and Gibbs plots revealed that the major mechanisms controlling the aquifer groundwater in Ojo region are geological rock weathering and mineralization, with a minimal influence of saltwater intrusion. The piper trilinear diagram also revealed that none of the cation was dominant while the anions were strongly dominated by HCO_3^- (weak acids). The hydrogeochemical facies which describes the geochemical characteristics of the groundwater were classified into 3 types; "Ca^{2+}–Mg^+–HCO_3^- (65 %)", "mixing zones (30 %)", and "Na^+–K^+–Cl^-–HCO_3^- (5 %)". The hydrogeochemical modelling revealed that the groundwater is characterized by forward cation exchange, while rock–water interactions (silicate dissolution) were heavily involved in the geochemical processes. The single pollution index showed that Pb, Ni, and Mn contributed significantly to contamination, and the multi–pollution indices showed that the groundwater was slightly-moderately polluted. The integrated groundwater quality index revealed that only 10 % were clean, 50 % were poor or moderately unclean, 30 % were highly unclean, and only 10 % were extremely unclean (unfit for utilization). The water pollution index showed that 70 % of the groundwater was good. The irrigation indices suggest that the groundwater would enhance soil quality and support plant growth. Multivariate analysis revealed that the groundwater is being influenced by geogenic factors and anthropogenic activities. The

* Corresponding author.
E-mail addresses: maliktoheeblekan@gmail.com (T.L. Jolaosho), adejuwon.mustapha@yahoo.com (A.A. Mustapha).

https://doi.org/10.1016/j.heliyon.2024.e38364
Received 28 May 2024; Received in revised form 23 September 2024; Accepted 23 September 2024
Available online 26 September 2024

health risk assessment (Hazard Quotient and Hazard Index) showed that exposure of adults to the investigated groundwaters could result in noncarcinogenic adverse effects. The cancer risk values also exceeded the minimum limit (1.0×10^{-6}) and thresholds (1.0×10^{-4}) for adults, indicating the carcinogenic potential of the groundwater.

1. Introduction

Groundwater is an indispensable resource required for human livelihood and sustainability—accounting for approximately 67 % of the available freshwater resources in several locations on earth [1]. Globally, groundwater resources have long been considered a benchmark for water purity due to their perceived cleanliness and safety [2]. Generally, water is crucial for maintaining human life, yet contaminated water is capable of causing a wide range of health-risk diseases. Numerous studies have demonstrated that even though groundwater may seem pure, it may contain a range of emerging pollutants [3–6]. Water quality degradation has undoubtably led to the disruption of ecological equilibrium coupled with the impairment of some environmental matrixes [7]. Hydrological processes such as deep percolation or groundwater recharge sources due to seasonal changes, geological setting, the mineralogical nature of watersheds or aquifers, interactions between water and rock, which include redox reactions, mineral dissolution, and ion exchange, as well as the elevated degree of potentially toxic metals due to geogenic and anthropogenic processes, have impacted the quality of groundwater required for human consumption and agricultural development, resulting in low crop yields due to poor irrigation events [8,9]. Water has the capability to completely dissolve and interact with the inorganic and organic residues of the soil that plants depend on for survival [10]. This demonstrates that the chemical constituents of groundwater could directly impact the physico-chemical components of the soil. Moreover, the nutrients obtained by plants as a result of water–soil interactions depend on water chemistry and the mineral composition of the soil [11].

The majority of undeveloped and developing nations face difficulty of accessing adequately clean water resources due to their depleted economies [12,13]. In addition, public health unawareness and inefficient environmental management policies have led to high levels of improper disposal of hazardous industrial and household wastes, particularly in undeveloped and developing nations [14]. These wastes make their way into groundwater, rivers, and other waterways. The consequences of these unsustainable activities include water–borne illnesses, especially typhoid fever and cholera, which are becoming more prevalent in African nations [15,16]. It was reported that more than 3.4 million Africans, especially children, die annually due to the consumption of polluted water [17,18]. However, due to recent technological developments, environmental orientations, and the implementation of several management policies, the issues of lack of access to clean waters have partially subsided. Nigeria is equally making great efforts to provide clean drinking water, especially in marginalized or less developed localities where the majority of residents rely on groundwater and surface waters for survival [19]. Nigerian governments have enacted several initiatives that stimulate the compulsory provision of healthful water, especially for people in marginalized areas [20]. Although the implementation of these regulations has been hampered by inadequate monitoring, this signifies that Nigerians are still facing challenges in accessing clean, drinkable water. Thus, continuous monitoring of groundwater is required to ensure that the available water is fresh and of high quality.

The comprehensive evaluation of groundwater in relation to its contamination degree and suitability for consumption and irrigation purposes requires an understanding and the application of one or multiple integrated metrics such as the groundwater quality index (GWQI), Nemerow multifactor, heavy metal pollution index (HPI), and irrigation index [21,22]. Studies on groundwater hydrochemistry revealed that the presence or distribution of chemical ions such as Cl^-, Mg^{2+}, NO_3^-, Na^+, SO_4^{2-}, K^+, HCO_3^-, and Ca^{2+} in groundwater in a particular geographical location are indicators of water type, facies, and quality, as well as the geological composition of such an area [23–25]. Similarly, the concentrations of heavy metals such as As, Cd, Cr, Cu, Hg, Fe, Ni and Zn have been utilized to estimate the pollution status of groundwater resources [26–29]. Overall, determining and understanding groundwater parameters is crucial to ascertain the suitability of groundwater for use and the source of its origin [30,31]. Water quality assessment can be done either via modern or conventional methods. Mohammed et al. [32] argued that the former is more efficient and reliable since the latter approach depends solely on comparing the evaluated water parameters with the established standard limits, in addition to the associated cost and time ineffectiveness. Several multivariate based techniques such as hierarchical clusters, factor analysis, Pearson correlation matrix, and hydrogeochemical models such as Gibbs and Piper trilinear diagrams, Scholler plots, and interionic molar ratios have been globally utilized by researchers to quantify the hydrogeochemical evolution and facies, water types, rock–water interactions, ionic exchange processes and reactions, hidden linear relationships, and potential sources of groundwater parameters in aquifer system [6,31–34].

Ojo District is a coastal region in the southwestern part of Nigeria. This area serves mainly as a residential and agricultural setting for a large number of people but is also known to house numerous industries. As a result, the inhabitants depend heavily on groundwater resources for several purposes, particularly for consumption, industrial and agricultural activities. Interestingly, the geological setting of Ojo region is structured in a complex form where the aquifer system shares hydrological boundaries with nearby freshwater and marine ecosystems. This enables salt deposits from the southern Atlantic Ocean and inland lagoons in flood plains to constantly interact, mix and consequently influence the aquifer systems in this region. Thus, this study becomes essential for a clearer understanding of the hydrological processes regulating the aquifer system in Ojo region. A comprehensive understanding of the geological characteristics of aquifer system in the study region would be crucial for efficient groundwater management and sustainability. More importantly, the intensive activities of a large steel industry (Volkswagen assembly plants) in this area have been perceived to contaminate and impair the quality of water in this region [35]. Despite these events, it is worrisome that no literature is

available on the hydrogeochemical properties and pollution status of groundwater systems in the Ojo district. This indicates that explicit and significant research gaps need to be covered in this region. The prevalence of other human-induced activities, particularly pesticide use for agricultural practices in Ojo district make this study relevant [35,36]. Additionally, investigating the groundwater chemistry in relation to the quality and contamination levels is crucial for the efficient implementation of conservative and management measures and policies for groundwater sustainability. To this end, this study intends to investigate the following: (i) Evaluate the physicochemical and hydrogeochemical characteristics of groundwater and also the ionic exchange processes and mechanisms regulating the hydrology and geochemistry of groundwater in alluvial aquifers via the application of integrated geochemical modeling tools; (ii) Examines the heavy metal concentrations in groundwater and compare with the maximum allowable limits recommended by international standard organizations; (iii) investigate the degree of groundwater toxicity and suitability for consumption and irrigation practices; and (iv) Determine the source apportionment and human health implications of the groundwater variables.

Overall, this study makes an attempt to offer novel viewpoints—attributions and optimizations that are suitable for the regional, global, and social contexts—to effectively manage groundwater infrastructure. To achieve our objectives, this study integrates hydrogeochemical techniques, the entropy water index, chemometrics, pollution–based indices, and health risk analysis. The long–term integrity of groundwater resources as well as the continued existence of the local community depend on the results of this study. This study provides a solid scientific basis and crucial insights that can help policymakers put necessary measures in place to protect the groundwater supply and guarantee effective management of water quality. The multifaceted approaches of the present study promise an improved understanding of the evolutionary processes and pollution constraints associated with aquifer groundwater in Ojo district. In addition, integrating the aforementioned methods will improve the precision of our findings and also offer comprehensive research insights.

2. Study area description

2.1. Geographical and socioeconomic characteristics

Ojo District is a coastal metropolitan area, with surrounding communities to the north and the Atlantic Ocean to the south. Ojo is

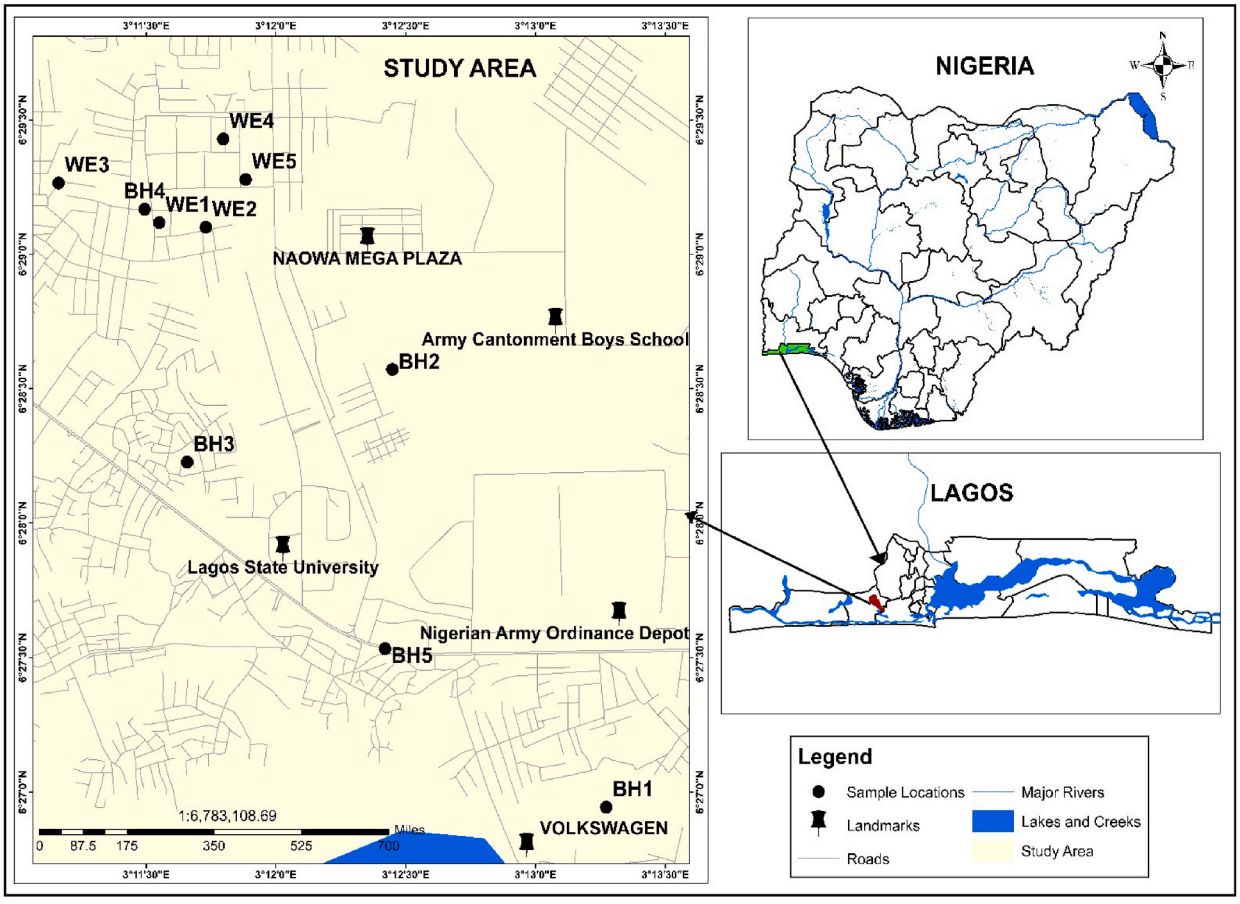

Fig. 1a. Map of Ojo district and its surrounding environment showing the sampled groundwater points.

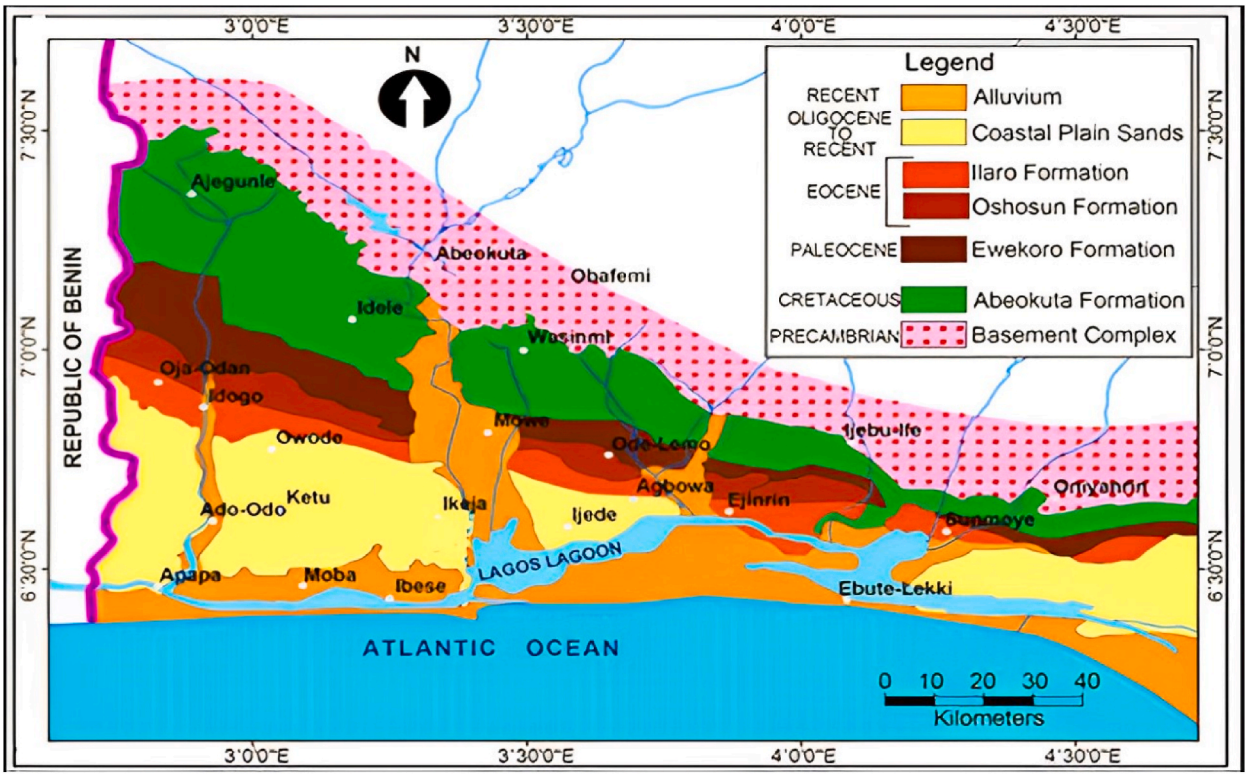

Fig. 1a. (*continued*).

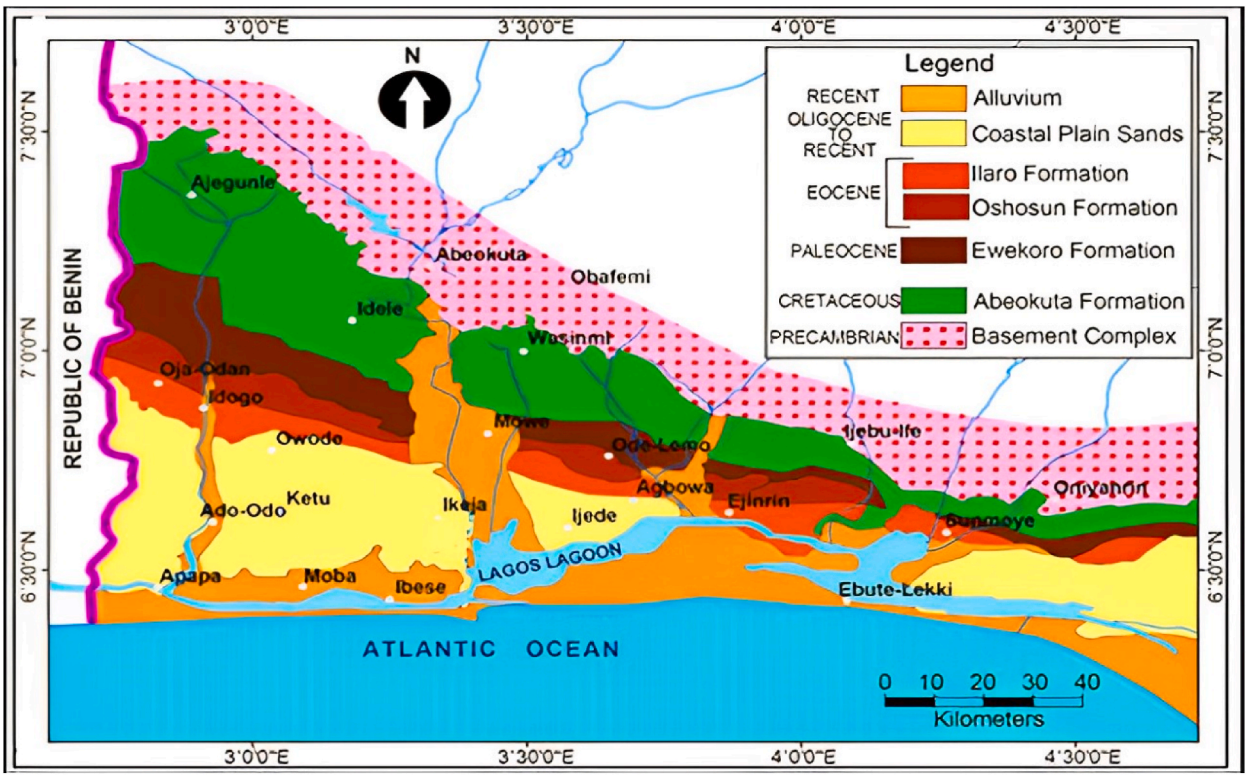

Fig. 1b. Map showing the geological and the stratigraphic columns within the eastern Dahomey basin.

located in the southwest region of Nigeria, between latitudes 6.49°N and 6.42°N and longitudes 3.18°E and 3.24°E. The specific coordinates of each of the sampled groundwater are provided in Supplementary Table S1. Over 900,000 people live in the Ojo district, and many parts of it have direct access to highways [37]. The study area holds significant cultural importance as it was among the first places in Nigeria where European merchants and missionaries made contact with natives. Its advantageous location near the coast and close to the city of Lagos has enabled the growth of a number of industries, most notably in the agriculture and automotive sectors, which are essential for creating jobs locally and boosting the economy of Lagos as a whole. There are over twenty established local industrial facilities in Ojo district, but the Volkswagen assembly plant (Fig. 1a) is the region's main attraction. The Volkswagen assembly plant is a major player in Nigeria's automotive sector. This plant is a component of a larger initiative that strengthen regional manufacturing capacity and lessen dependency on automobile imports. The production and processing of steels for use in automobiles, construction and other industrial applications are among the many activities carried out by Volkswagen steel facility. Products like plastics, powder metallurgy, paper milling, textile coating, and household materials are also produced by other nearby industries. Additionally, agricultural activities are being practiced extensively by farmers in Ojo district. As a result, agro-industrial factories produce agrochemicals that are largely used by farmers for agricultural activities. Consequently, this frequently exposes the area to a wide range of environmental contaminants. Other institutional establishmentss in Ojo district include the Cantonment, which is one of the biggest military barracks in West Africa in terms of land mass, and Lagos State University (Fig. 1a).

2.2. Geological and hydrogeological profiles

Lagos State is considered a coastal region with quintessential hydrological terrains located within deposition points, where upstream water systems such as lagoons, canals, creeks, streams, and tributaries drain predominantly into Lagos Lagoon and eventually deposit in the southern Atlantic Ocean (Fig. 1b). This study area is geographically established within the Dahomey Basin (Fig. 1b) on stratified layers of sedimentary rocks composed of clay, silt, and sand of different types, forms, and mineral compositions [38,39]. The Dahomey Basin extends to the Okitipupa Ridge, also known as the Ilesha Spur, and the Volta Delta ecosystem in the southwestern parts of Nigeria and Ghana, respectively. It is made up of a large wedge of Eocene, Paleocene, Cretaceous, and Precambrian sediments (Fig. 1b) that build up substantially from the basin's onshore edge—where the majority of the sediments are clastic—to the offshore, where thicker, fine–grained Cenozoic sediments cover the Cretaceous rocks that formed in leptogeoclinal basins [39,40]. In the investigated location, the surface sand is composed of fine–grained porous materials such as grit sand deposited by littoral and barrier beaches. Occasionally, the enlisted geological mineral deposits are interbedded with peat and vegetable remnants. Although sandy alluvial deposits and clay represent the two fundamental lithologic materials revealed by the subsurface geology of this area, but the presence of unconsolidated sands and clayey with subordinate shale (Ilaro formation), sandstones, tributary gravels, and salt deposits can be clearly visualized in various subdivision layers of the investigated region as illustrated in Fig. 1b [39–41]. It is generally recognized that the lithological attributes of this region affect the flow of groundwater. This is because the permeable nature of sandy alluvial deposits such as clay lenses, coarse sand, and small pebbles allows for good groundwater flow. In addition, the upper strata of this area contained sandstones and gravels. The increased permeability rates of these materials also aid in groundwater movement. On the other hand, the existence of clay layers serves as a confining unit, limiting groundwater movement and generating pressure differentials that modify the flow regime.

Due to the differences in the permeability of sandy alluvial and clayey layers, groundwater flows in an intricate pattern in which less permeable layers obstruct vertical movement and move laterally along permeable layers [42]. In Ojo region, sand and gravel soils act as recharge compartments, allowing rain and seawater to seep in and replenish groundwater supplies because of the high permeability characteristics [43]. The presence of these impermeable layers frequently leads to localized flow directions, which often result in the accumulation of groundwater and the formation of perched aquifers. Since Ojo District is coastal, being close to the ocean and other lagoon systems has brought about frequent saltwater intrusion, particularly in some areas of the study region where groundwater was over–extracted.

Ojo has a wide range of aquifer characteristics, including yield. According to reports, the groundwater yields in Ojo region typically fall between 5 and 30 L per second, though localized factors sometimes cause variations [44,45]. Furthermore, the transmissivity of sandy aquifers varies between 5 and 50 m^2/day, whereas the transmissivity of more consolidated clay–rich areas is much lower. In the study region, the storativity in unconfined aquifers typically ranges from 0.05 to 0.25 (5 %–25 % of the aquifer's volume), but because of the pressure conditions in confined aquifers, values may be lower [46]. The Hydraulic conductivity, which describes the ease with which water can move through pore spaces, typically ranges from 10^{-3} to 10^{-5} m/s in sandy layers, while clay layers have much lower hydraulic conductivities, often $<10^{-7}$ m/s in the study region [46]. The major source of recharge in Ojo district is rainfall, whereby the aquifers are replenished by a substantial amount of annual precipitation. Similarly, nearby lagoons, rivers, and streams, as well as urban runoffs (if not directed into drainage systems) also facilitate groundwater recharge through infiltration, particularly during the rainy season. The commercial agricultural activities in this area benefit from irrigation practices that also improve local groundwater recharge. Conversely, evapotranspiration, natural springs, extraction or pumping for home, industrial, and agricultural uses, coastal processes, and tidal influence are the sources of groundwater discharge in this area.

The groundwater in this region is categorized into four (4) basic aquiferous layers based on quality and characteristics. The first layer extends up to 12 m below ground level and consists of clay and sand. Due to the limited depth, this layer is susceptible to contamination, although it is of minor importance for groundwater supply. The second and third aquifers lie between 20–100 m and 130–160 m below sea level, respectively. The fourth aquifer is about 450 m below the seal level and is composed of a thick layer of shale [38]. Geophysical information as well as drilling exploration data demonstrate that the aquifer system within the study region is confined.

3. Materials and methods

3.1. Water collection and preservation techniques

Groundwater samples were collected from ten (10) randomly selected boreholes (BH) and hand-dug wells (WE), with approximate depths of 25.8 m (BH1), 24.5 m (BH2), 20.7 m (BH3), 25.5 m (BH5), 23.4 m (WE1), 27.5 m (WE2), 23.2 m (WE3), 24.8 m (WE4), and 28.5 m (WE5) in the second layer of the aquifer for three (3) months (March to May 2023). The random selection method was used to ensure that the experimental survey included all of the groundwater resources in the Ojo district. Samples were procured in replicates from the selected groundwater (Fig. 1a) to ensure the authenticity and quality of the samples. Acid-free sampling bottles (1.5 L) were utilized to obtain samples. Each piece of glassware was cleaned and dried. Prior to water collection, the bottles (Corning Gosselin) were washed with soap free of toxicants and eventually soaked in 10% HNO_3. To maintain the initial grade of the groundwater, the collected samples were acidified with 0.5% HNO_3 in well-labeled bottles (BH1–BH5 and WE1–WE5) and were stored at room temperature (4 °C) prior to laboratory evaluation.

3.2. Preparation of the groundwater samples

Prior to the determination of heavy metals, filter paper (Whatman No. 41) was utilized to filter the collected samples (500 mL each). The samples were then acidified (1 mL, 65% HNO3). A total of 250 mL of the acidified solution was fixed in a graduated beaker and then heated on a hotplate until it was reduced to 25 mL via evaporation. The analysis was conducted to determine each heavy metal parameter, except for As, where 0.5 mL of KI and $C_6H_8O_6$ and 3 mL of HCl were fixed to the groundwater sample and kept for 2 h.

3.3. Quality control and assurance

To verify and ascertain the quality of the analysis, critical adherence to relevant standards and regulatory protocols was maintained. For optimal reliability and precision, each sample was examined in triplicate. Verification of the concentrations of the analyzed parameters was done using certified reference materials (CRM, Labmix–Tech, Al 99, USA). The qualitative solutions of 99.98 % (ultrahigh) of the required elements at the purification level collected from a medical system supplier (Varian Inc) in the USA were used. The chemicals used were from Germany (E. Merck). In accordance with the stock solution guidelines (conc. of 1000 mg/l), the standard solutions were prepared with filtered distilled water. This assessment was dependent on the calibration curves (CC), plotted at five different concentrations (0.050, 0.100, 0.200, 0.250, and 0.300 mg/l). Before conducting the sample analyses, runs were carried out for each parameter to determine the correlation coefficient (r^2) values on the CC. To ensure high–quality analyses, extensive washing was carried out repeatedly and the blank samples were also examined. The intensity data of the standard and blank samples were utilized to ascertain the detection limits of the apparatus, and high recovery rates (92.3%–99.2 %) were obtained. The detection limits (LOD) and limit of quantification (LOQ) were: Na^+ (0.0153 and 0.0632), Mg^{2+} (0.0025 and 0.0133), Ca^{2+} (0.0122 and 0.0433), K^+ (0.0012 and 0.0267), SO_4^{2-}, NO_3^- (0.0048 and 0.0145), Cl– (0.0025 and 0.0389), HCO_3^- (0.0042 and 0.0139), As (0.0027 and 0.0154), Cd (0.0056 and 0.0184), Cr (0.0038 and 0.0167), Cu (0.030 and 0.0172), Fe (0.0094 and 0.0205), Pb (0.0013 and 0.0136), Mn (0.0048 and 0.0183), Ni (0.0022 and 0.0137) and Zn (0.0099 and 0.0221). All the evaluated groundwater parameters were expressed as mg/l.

3.4. Determination of the physicochemical, hydrogeochemical and heavy metal parameters

For water quality tests, the chemicals procured and used were of analytical grade. The reagents used were purchased from the US Company Hach Chemical. An electrode tool (version: IONIX PC–50) for multiple parameters was adopted to measure the pH, Total Dissolved Solids (TDS), Electrical Conductivity (EC), and Total hardness (TH) of the unfiltered water using the standard procedure (APHA, 2005). The biological oxygen demand (BOD) was determined from the dissolved oxygen (DO) content in 60 ml aliquots of the samples prior to and following 5 days of incubation under dark conditions at 20 °C. The chemical oxygen demand (COD) was evaluated using an enclosed reflux, colorimetric method, and 2 ml aliquot of an evenly distributed sample was digested with the dichromate/sulfuric acid COD reagent in a reactor (Grant QBD 2) at 150 °C for 2 h. The electrode was carefully cleaned with distilled water and then gently wiped with dry tissue paper prior to reading. The hydrogeochemical parameters [cations (Mg^{2+}— K^+—Ca^{2+}—Na^+) and anions (SO_4^{2-}—NO_3^-—Cl^-—HCO_3^-)] were determined using the ion chromatography (IC) method except for HCO_3^- which was determined through the water titration technique with H_2SO_4. The ions were separated from one another and detected using an ion self–producing suppressor integrated with conductivity sensor. Heavy metal analyses for the nine (9) parameters (As, Cd, Fe, Cu, Cr, Zn, Ni, Pb, and Mn) were done with the aid of a flame atomic absorption spectrophotometer (AAS) (Varian AA 240). A hydride–producing device (VGA–77) and analytical software (version 5.01) were both used to improve the efficiency of the instrument.

3.5. Hydrogeochemical modeling

Schoeller plot was generated to illustrate the relative concentrations of the distributed hydrogeochemical ions while the piper diagram was generated to identify the dominant water type, hydrogeochemical facies and correlative contents of the major chemical ions and to provide clear reflections on the fundamental geological processes required to comprehend the chemical hydrology of the groundwater [9]. Both plots utilized the cation and anion variables, expressed in milliequivalent (meq/l). The top layer of the diamond

in the Piper trilinear plot represents groundwater with high concentrations of Ca^{2+}, Mg^{2+}, Cl^{-}, and SO_4^{2-} ions, denoting permanent hardness. The groundwater samples depicted in the left side are enriched with Ca^{2+}, Mg^{2+}, and HCO_3^{-}, indicating temporary hardness. Alkaline bicarbonate (Na^{+}, K^{+} and HCO_3^{-}) is represented at the base of the diamond structure–like plot while the salt deposits (Na^{+} and Cl^{-}) are primarily visible in the right part of the diamond–shaped structure. The Gibbs diagram, on the other hand, was used to assess the relationship between the lithological and hydrogeochemical processes in the groundwater aquifer system [9]. Aquachem software (version 3.7) was used to prepare the piper trilinear diagram, while Schoeller and Gibb's diagrams were plotted on Excel spreadsheets.

3.6. Contamination assessment of groundwater resources

3.6.1. Single factor pollution index (Pi)

The Pi is an essential model for evaluating the significance contamination effects of individual metals on water. The Pi was computed from equation i:

$$\mathrm{Pi} = \frac{\mathrm{Ci}}{\mathrm{Si}} \tag{1}$$

Where Ci (mg/l) = estimated individual metal; and Si (mg/l) = regulatory standard limits of metals and are provided in Table 3.

The Pi values are classified as follows; (a) $\mathrm{Pi} \leq 1$ (no contamination) (ii) $1 < \mathrm{Pi} \leq 2$ (low contamination degree); (iii) $2 < \mathrm{Pi} \leq 3$ (moderate contamination) and (iv) $\mathrm{Pi} > 3$ (extremely high contamination), which denotes environmental risk and such water is considered unsuitable for consumption except when treated [47,48].

3.6.2. Nemerow multifactor index (Y_N)

$$\mathrm{Y_N} = \sqrt{\frac{(\mathbf{max}\ \mathrm{Yi})\text{^}\mathbf{2} + (\bar{\mathrm{Y}})\text{^}\mathbf{2}}{\mathbf{2}}} \tag{2}$$

Where Y_i = heavy metal with the maximum concentration in a group; and $\bar{Y}$ = average value of one heavy metal in a computed dataset.

The Y_N categories are shown below.

$Y_N \leq 1$ (not polluted); $1 < Y_N \leq 2.5$ (slight pollution); $2.5 < Y_N \leq 7$ (moderate pollution); $Y_N > 7$ (high pollution) [48].

3.6.3. Contamination degree (C_{degree})

The C_{degree} is one of the most frequently used indices for discerning the comprehensive effects of toxicants in water resources [49,50]. This index is a two-step technique, as it first assesses the pollution status of a single pollutant (contamination factor) in respect to its regulatory limit, then aggregating or summing the contamination values over the whole number of the estimated pollutants. In this study, the C_{degree} was employed to determine the extent of groundwater pollution in the Ojo district. The C_{degree} was computed via equations iii and iv.

$$\mathrm{Cfi} = \frac{Cmi}{Cni} - 1 \tag{equ iii}$$

$$\mathrm{C_{degree}} = \sum_{i=1}^{n} [Cfi] \tag{equ iv}$$

Cfi = contamination factor; Cmi = level of individual metal in groundwater system; Cni = regulatory limits of heavy metals based on international standard recommendation and are illustrated in Table 3; n = total count of the metals analyzed in this study. The rating of the C_{degree} values is based on three categories; (i) $C_{degree} < 40$ (low or no contamination) (ii) C_{degree} of 40–80 (moderate contamination) and (iii) $C_{degree} > 80$ (high degree of contamination)

3.6.4. Heavy metal pollution index (HPI)

The HPI is a crucial ecological modeling parameter for comprehensive monitoring of water contamination status based on the concentration of heavy metals present [51]. The HPI serves as an indicator for detecting the contributions of both individual and cumulative toxic metals in water. This index assigns weighted unit values to individual metals based on their proportional contribution to water contamination. The HPI is derived from the equation below.

$$HPI = \frac{\sum_{i=1}^{n} [Wu.Qi]}{\sum_{i=1}^{n} Wu} \tag{equ v}$$

Wu = computed relative weight units of each parameter (Table S2); Qi = the subindex of each variable, and n = is the total count of heavy metals used for the assessment. The equation (vi) provided below was used to compute the Qi.

$$Qi = \frac{(Cx - Zi)}{(Mx - Zi)} \times 100 \quad \text{(vi)}$$

Cx = concentration of a single metal; Zi = ideal value of a single metal; Mx = allowable limits in water.

The HPIs were classified into three classes. The HPI value below 100 (<100) denotes low or no contamination, while a HPI value of 100 (=100) denotes the threshold or maximum limit, indicating average or moderate contamination. Finally, the HPI value above 100 (>100) indicate extreme contamination, which suggests that such water is unfit for utilization, particularly consumption [35,47].

3.6.5. Modified heavy metal index (MHI)

The MHI also considers the ecological risks associated with heavy metals in groundwater resources and was derived after slight modifications to the HPI [51]. In this study, the MHI was employed to ascertain the probabilistic health implications and overall adverse effects of heavy metal pollution in groundwater at a specific location. In an attempt to compute the MHI values, three (3) mathematical procedures were adopted. (i) Weightage unit values were assigned to the heavy metals (Table S2), based on their toxicity influence (ii) The second and (iii) third procedures were achieved via equations (vii) and (viii), respectively.

$$MHMI = \sum_{i=1}^{n} \frac{(Wu.Ci)}{Si} \quad \text{(equ vii)}$$

$$\mathrm{Wu} = \frac{Wi}{\sum_{i=1}^{n} Wi} \quad \text{(equ viii)}$$

n = total count of the analyzed metals. Ci = level of metal in groundwater; Wu and Wi = assigned and relative weightage units; Si = allowable limits (Table 3)

3.7. Assessment of suitability for drinking and irrigation purposes

3.7.1. Groundwater quality index (GWQI)

The GWQI is considered a rating system that employs physicochemical and heavy metal variables to generate the outcomes required to provide clear reflection and ascertain the overall groundwater quality to determine its aptness for usage, especially for drinking [32,34,52]. By using this method, the multidimensionality of the groundwater data sets is reduced to a dependent numerical value. The GWQI was computed with the aid of the assigned weightage units (Wi), rating scale and accumulating subindices. In this study, twelve (12) hydrogeochemical parameters (EC, TDS, pH, TH, Mg^{2+}, Na^{+}, Ca^{2+}, K^{+}, SO_4^{2-} NO_3^{-}, Cl^{-} and HCO_3^{-}) and nine (9) heavy metal variables (Cu, Ni, As, Cr, Zn, Cd, Pb, Fe, and Mn) were considered for the GWQI assessment. The exclusion of temperature, BOD and COD parameters was due to the nonavailability of assigned weightage units (Wi). The procedures below were employed to estimate the GWQI.

Step–I: Subindex rating of each groundwater parameter from equation (ix).

$$Q_i = \frac{\mathrm{xa} \times 100}{\mathrm{Xs}} \quad \text{(equ ix)}$$

Xa = measured value of a parameter; Xs = proposed standard limit of a parameter.

Step–II: The relative weightage unit (Wu) of each groundwater parameter was computed via equation (x):

$$W_u = \frac{\mathrm{Wi}}{\sum_{i=1}^{n} \mathrm{Wi}} \quad \text{(equ x)}$$

Wi represents the assigned weightage units of each parameter and is presented in Table S2.

Step–III: Computation of the GWQI values from the following formula:

$$\mathrm{Sw} = \mathrm{W_u\ x\ Q_i} \quad \text{(equ xi)}$$

$$\mathrm{GWQI} = \sum \mathrm{Sw} \quad \text{(equ xii)}$$

For the purpose of reducing the disparity of the highest level of each rating as well as the lowest level of the following rating, the GWQI classification scale as suggested by Tyagi et al. (2013) was used and is depicted in Table S3.

3.7.2. Water pollution index (WPI)

The WPI, developed by Hossain and Patra [53], is considered a feasible and effective index for broad evaluation of the contamination levels of water in relation to the presence of different pollutants. Ever since its invention, this index has been adopted by several researchers on both global and local scales for critical evaluation of water resources in relation to suitability for usage [26–29]. There are a number of important reasons for its widespread acceptance, but the most appealing is its simplicity and directness. Two steps are involved when computing the WPI values and are described below. The equation (xiii) was used to compute the WPI values of all the groundwater variables except for pH which requires some modifications as shown in equations (xiv) and (xv). The equation (xiv) was

used to compute the PLi of samples with pH values below 7, while the equation (xv) was for samples with pH values above 7 [53].

3.7.2.1. 1st step. Determination of the pollution load of each parameter via equation (xiii)

$$PLi = \frac{1 + (Mz - Al)}{Al} \quad \text{(xiii)}$$

$$PLi = \frac{(Mz - 7)}{Alx - 7} \quad \text{(xiv)}$$

$$PLi = \frac{(Mz - 7)}{Aly - 7} \quad \text{(xv)}$$

Mz = concentration of a measured variable; Al = allowable limit of each variable except for pH; Alx = proposed value of pH below 7 and is 6.5; Aly = proposed value of pH above 7 and is 8.5.

2nd step. The PLi scores of each variable under examination were summed, and the total number of variables was divided by the resulting total to determine the groundwater WPI ratings (equation xvi). It is important to stress that a parameter should not be taken into account in the total count (n) calculation for a sample if its value is zero. The rating scales used to interpret the WPIs are provided in Table S3.

$$WPI = \frac{1}{n} \sum_{i=1}^{n} PLI \quad \text{(xvi)}$$

3.7.3. Assessment for irrigation purposes

To preserve soil health and increase crop productivity, irrigation water quality is crucial. Both the physical conditions of the soil and crop yields can be impacted by the features of irrigation water [54]. Irrigation indices are specific measures or indicators that are mainly used for assessing the efficiency, sustainability, and impact of groundwater usage for irrigation practices [55,56]. These indices are designed to evaluate the relationship between the amount of groundwater used for irrigation and the resulting effects on plant yield, and overall soil ecosystem health. Given that agricultural activities are common within the study area, it is essential to ensure that groundwater resources are managed effectively and sustainably for farming practices. To determine whether the groundwaters under consideration are suitable for use in irrigation, a number of irrigation indices provided in Table 1 were used.

3.8. Health risk assessment (HRI) of heavy metals in groundwater

The HRI is the procedure for estimating the likelihood that a specific unfavorable health effect will materialize during a specific time or period. This study employed several risk metrics [average daily dose (ADD), reference dose (RfD), hazard quotient (HQ), hazard index (HI), and cancer risk index (CRI)] to calculate the adverse effects of the analyzed heavy metals in groundwater in exposed population. The HRI of this study considered children and adults, since both age categories are expected to be susceptible to exposure in this residential neighborhood over an extended period of time.

3.8.1. Average daily dose (ADD)

The ADD values were determined using the equation below:

$$ADD_{ingestion} = \frac{Ct \times DI \times EF \times ED}{BW \times AT} \quad \text{(equ xvi)}$$

Table 1
Parameters used for estimating the suitability of groundwater resources for irrigation practices.

Indices	Formula	Rating Scale	Interpretation	References
Sodium adsorption ratio (SAR)	$SAR = \frac{Na^+}{\sqrt{Ca^{2+}+Mg^{2+}+Na^+/2}}$	0–10 11–17 18–26 >26	Excellent Good Doubtful Unsuitable	[57]
Permeability Index (PI)	$PI = \frac{Na^+ + \sqrt{HCO3^-}}{(Ca^{2+} + Mg^{2+} + Na^+)} \times 100$	>75 % 25 %–75 % <25	Class I (Excellent) Class II (Good) Class III (Bad)	[58]
Soluble Sodium Percent (SSP)	$SSP = \frac{Na^+}{(Ca^{2+} + Mg^{2+} + Na^+)} \times 100$	<60 >60	Suitable Unsuitable	[59]
Magnesium hazard ratio (MHR)	$MHR = \frac{Mg^{2+}}{Ca^{2+} + Mg^{2+}} \times 100$	<50 >50	Suitable Unsuitable	[60]
Kelly's Ratio (KR)	$KR = \frac{Na^+}{Ca^{2+} + Mg^{2+}} \times 100$	<1 >1	Good Bad	[61]

Note: The ionic variables used are expressed in meq/l.

$$ADD_{dermal} = \frac{Ct \times ABS \times EF \times ED \times ET \times SA \times CF \times K_p}{BW \times AT} \quad \text{(equ xvii)}$$

Where Ct (mg/l) = estimated values of a single toxicant; ABS = dermal absorption factor (unitless); DI (L/day) = water consumed on a daily basis; EF (days) = exposure frequency; ED (years) = exposure period; CF = conversion factor (cm^3); ET (h/event) = exposure time; SA (cm^2) = vulnerable part of the skin to contact; Kp (cm/hour) = dermal permeability coefficient [As = 0.003; Co = 0.0004; Ni = 0.0002; Zn = 0.0006; Cd = 0.001; Pb = 0.001; Cr = 0.002; Cu = 0.001; Mn = 0.001; Fe = 0.001 (mg/kg/day)] [35,36,74]; and BW (g) = body weight, and AT (days) = EF x ED (noncancer and cancer risk). Other standard values necessary for the risk assessments are presented in Supplementary Table S4.

3.8.2. noncarcinogenic risk evaluation

The noncancer parameters (HQ and HI) are essential indices that are widely utilized for calculating the full exposure of water to a set of contaminants that have been identified or are potentially present in that location. These indices were employed to decipher the overall noncancer implications associated with heavy metals in groundwater. The equations below illustrate how the HQ and HI values were computed.

$$HQ_{ingestion} \text{ and } HQ_{dermal} = \frac{ADDingestion}{RfDingestion} \text{ and } \frac{ADD\ dermal}{RFD\ dermal} \quad \text{(equ xviii)}$$

$$HI = \sum_{i=1}^{k} HQingestion + HQdermal \quad \text{(equ xix)}$$

HQ, ADD, RfD and HI have been previously described. The RfD values are presented in Supplementary Table S5.

The HQ value of above 1, implies risk from a single heavy metal in groundwater. Human health is considered to be at noncarcinogenic risk as a result of consuming two or more heavy metals in groundwater above the allowable limits. Noncancer risk can occur when the HI exceed 1 (HI $>$ 1), conversely the HI value below 1 demonstrate an acceptable range for safety [35,62,74]. Thus, noncarcinogenic risk is categorized based on the provided rating scale. (i) negligible (risk level 1; HI $<$ 0.1), (ii) low risk (risk level 2; HI $\geq$ 0.1 $<$ 1), (iii) medium risk (risk level 3; HI $\geq$ 1 $<$ 4) and (iv) extreme risk (risk level 4; HI $\geq$ 4) [23,63].

3.8.3. Carcinogenic risk evaluation

The carcinogenic risk index is commonly used for determining the anticipated cancer concerns as a result of exposure to carcinogens. The cancer risk (CR) and the lifetime cancer risk (LCR) were utilized to determine the likelihood of an individual developing one or multiple forms of cancer due to chronic exposure to carcinogens, for a certain number of years. The international agency research for cancer (IARC) has classified four (4) heavy metals [As, Cd, Cr, and Ni] as more prevalent (category 1) carcinogens, because they are estimated to be the most significant cancer–causing metals [64]. Pb has also been identified as an element with possible carcinogenic potential. The equations below were employed to compute the cancer risk values in groundwater.

$$CR\ (\text{ingestion and dermal}) = ADD_k \times SF_k \quad \text{(equ xx)}$$

Where CR = possibility risk of a single carcinogen; ADD_k = average daily dose of one carcinogen; SF_k = slope factor of each carcinogen and are stated in Table S5.

The lifetime cancer risk (LCR) was computed from the equation below

$$LCR = \sum_{i=1}^{k} CRingestion + CRdermal \quad \text{(equ xxi)}$$

For CR and LCR, the minimum and maximum (threshold) limits are 1 x 10^{-6} and 1 x 10^{-4} respectively [35,36]. The value higher than the threshold implies the chance or likelihood of a person experiencing cancer adversity. It is worthy to note that 1 x 10^{-6} signifies the lowest risk value i.e 1 out of 1000000 while 1 x 10^{-4} represents the highest exposure levels, inferring 1 out of 10,000 individuals, prior to health severity [62,65]. If the computed values are greater than the previously specified threshold limits, additional chemical assessment will be taken into consideration. Conversely, lower values below these thresholds suggest that cancer incidence is unlikely and no additional risk assessments of carcinogens are required [36,39].

3.9. Univariate and multivariate statistical analysis

Data evaluation, hydrogeochemical modeling, entropy water quality and pollution indices, chemometrics and risk assessments are crucial in this comprehensive study. The interpretations of the outcomes from these assessments are required to provide clear reflections of the status of the examined groundwater. To this end, univariate and multivariate techniques were adopted for critical assessment. For the univariate evaluation, the mean (average), maximum, and minimum values of the water parameters were calculated. In an attempt to identify the linear relationships and likely sources of the dominant water parameters, this study employed multivariate analyses. Pearson's correlation matrix, established at $P < 0.05$ and $P < 0.01$ (one tail test) was adopted to capture the linear relationship between associated variables. This matrix quantifies how well each component's variation may be accounted for by its correlation with the others [66]. R–mode factor analysis (FA) was performed to reduce the data set into a cogent form and to extract the principal components required to identify the possible source of origin of the evaluated groundwater parameters [36]. This study initially transformed the raw datasets using the centered log–ratio (CLR) before performing the FA to make sure they were consistent,

dependable, and systematically distributed. The dataset transformation was performed using the equation below [67].

$$\mathrm{CLR(x)} = [\log(x_1 / g\,(x))], \ldots\ldots\ldots\ldots, [\log(x_N / g\,(x))] \quad \text{(xxii)}$$

Where x = measured parameters of this study; g (x) = geometric mean of the parameters of x_1, and x_N; x_N = concentrations of each parameter

Kaiser–Meyer–Olkin (KMO) test and Bartlett test of sphericity (BTS) were also utilized to determine the appropriateness and sufficiency of the datasets for the analysis. Cluster analysis is considered as a potent classifying analytical tool that aids in grouping identified factorials in clusters based on identical chemical attributes. Centroid clustering combined with the squared Euclidean distance technique was utilized to generate factorial clusters based on affinities or differences in relation to chemical attributes. A dendrogram—a diagram that resembles a tree—was produced as a result of this chemometric method. Furthermore, the Z–score data standardization procedure was used to reduce statistical biases [68]. Statistical tools (version: IBM SPSS 16.0) were used for all analyses. Additionally, ArcGIS system was employed to develop the geological and geospatial maps necessary to identify the lithostratigraphic units, and spatial distrubtion patterns of the sampled groundwaters in the study location. This was accomplished by using the Kriging interpolation methods that incorporated hydrogeochemical and heavy metal datasets obtained from the groundwater samples.

4. Results and DISCUSSION

4.1. General physicochemical and hydrogeochemical characteristics of groundwater

Table 2 shows the summary of fifteen (15) physicochemical and hydrogeochemical parameters evaluated in groundwater samples from the Ojo district. In this study, the temperature levels ranged from 27.56 to 29.95 °C, with a mean value of 28.64 °C. These values were slightly higher than the 26.96–27.34 °C reported by Odu et al. [69] in groundwater. It has been reported that the temperature of an aquifer is also dependent on the depth, such that an increased depth influences a high temperature level [38]. This corresponds with the high temperature of 70 °C reported by Onwuka and Amadi [70] in borehole water taken from a depth of 750 m in Lagos State, compared to the shallow depth of 20–50 m examined in this study. Nonetheless, WHO (2008) affirmed that a temperature of 25–50 °C is optimal and safe, because it can prevent the growth of microorganisms in drinking water.

The pH values ranged between 5.55 and 6.35, with a mean value of 6.03, suggesting slight acidity in the aquifer groundwater. As shown in Fig. 2b, slightly acidic contents were obtained in all the groundwater samples, which might suggest the absence of calcareous rocks (limestones) and the presence of sandstones in the study area. It has been reported that limestones are highly enriched in calcite, which increases the pH (≥ 7) of soils, while sandstones are highly composed of silica, which reduces the pH of soil to neutral or slightly acidic (< 7). Moreover, the homogenous distribution trends of pH in the samples implied mutual interdependence during geochemical processes [67]. Nonetheless, the pH levels were below the 6.5–8.5 desirable limits recommended by WHO [71], signifying that the groundwater might be acid–contaminated.

The TDS is considered the most unique and reliable indicator of contaminated groundwater. It is influenced by the interaction between geological, hydrogeochemical, and biochemical particulates present within or flowing through an aquifer layer [72]. In the present study, the TDS concentrations ranged from 182.02 to 320.77 mg/l, with a mean value of 251.05 mg/l. These TDS values are 3–7 times below the standard value of 1000 mg/l recommended by WHO [71], which is considered suitable for drinking purposes. The significantly low TDS values obtained in borehole water samples are an indication of insufficient levels of essential minerals such as

Table 2
The minimum, maximum and mean concentrations of the groundwater parameters.

WQPs	Min	Max	Mean	SD	CV%	Standard limits ([a]SI)
Temp (°C)	27.56	29.25	28.64	0.57	1.98	**NA**
pH (at 25 °C)	5.55	6.35	6.03	0.24	3.95	6.5–8.5
TDS (mg/l)	182.02	320.77	251.05	70.13	27.94	1000
TH ($CaCO_3$ mg/l)	46.22	182.45	114.08	62.80	55.05	80–100
EC (μS/cm)	107.78	448.65	278.50	171.09	61.43	2500
BOD (mg/l)	0.89	1.75	1.23	0.30	24.45	5
COD (mg/l)	1.00	4.37	2.59	1.63	62.98	200
Na^+ (mg/l)	36.87	96.49	65.53	24.51	37.40	200
Mg^{2+} (mg/l)	11.09	16.87	13.28	1.83	13.77	150
Ca^{2+} (mg/l)	47.65	58.88	51.81	3.70	7.15	75
K+ (mg/l)	2.55	7.86	4.78	1.90	39.82	30
SO_4^{2-} (mg/l)	19.94	53.67	35.13	15.65	44.56	400
NO_3^- (mg/l)	15.15	44.25	28.17	12.36	43.87	50
Cl^- (mg/l)	20.43	27.16	23.26	2.05	8.79	250
HCO_3^- (mg/l)	64.13	125.82	96.67	19.06	19.72	250

WQPs (Water quality parameters), SCs (Sample codes), BH (Borehole water), WE (Well water), Temp (Temperature), EC (Electrical conductivity), TDS (Total dissolved solids), TH (Total hardness), BOD (Biological oxygen demand), COD (Chemical oxygen demand), min = *minimum,* max = *maximum, CV = coefficient of variation.*

[a] Si [71,75].

Table 3
Concentrations (mg/l) of heavy metals in groundwater from Ojo district.

HMPs	Min	Max	Mean	SD	CV	[a]Si
As	0.001	0.005	0.0026	0.001838	70.68743	0.010
Cd	0.001	0.003	0.0022	0.000919	41.76984	0.005
Cr	0.002	0.005	0.003	0.000943	31.42697	0.03
Cu	0.001	0.002	0.0012	0.000422	35.13642	1.50
Fe	0.11	0.27	0.186	0.050596	27.20239	0.30
Pb	0.001	0.03	0.0105	0.01203	114.572	0.01
Mn	0.003	0.16	0.0656	0.065332	99.59142	0.08
Ni	0.05	0.12	0.091	0.026437	29.05111	0.07
Zn	0.003	0.05	0.0211	0.019267	91.31204	4.00

* HMPs (Heavy metal parameters), Si (Maximum standard limits).
[a] *Si* [71,75].

Mg^{2+}, Ca^{2+}, Fe, Na^{+}, and K^{+} due to low rock–water interactions, which could result in unpalatable tastes, hardness, and corrosive states [73]. Another possible explanation for the relatively low TDS levels could be due to inadequate or a lack of feldspars in the geological materials (quartzitic sandstones) present in the study region. In addition, high differences in the concentrations of TDS in boreholes and hand–dug wells suggest heterogeneous distribution patterns (Fig. 2c).

The TH values in groundwater range from 46.22 to 182.45 mg/l, with a mean of 114.08 mg/l. Contrary to the TDS, the mean concentration of TH exceeded the desirable limits of 80–100 mg/l slated by WHO. In addition, approximately 50 % of the groundwater samples, which are mainly those from hand-dug wells, exceeded the maximum recommended limit (Fig. 2d). The concentrations of TH are directly related to the levels of Ca^{+2} and Mg^{+2} present in groundwater [32]. However, given the lithological characteristics of the study area (absence of calcite and dolomite), it is evident that other external processes, mainly human-induced, such as the application of Ca-Mg containing fertilizer for agricultural activities, discharge from local industrial facilities, runoff, and direct deposits from the ocean and other nearby lagoons, influenced the TH of the groundwater.

The EC levels of this study ranged from 107.78 to 448.65 (μS/cm), with an average value of 278.50 μS/cm. Although there is no universally agreed permissible limit for EC in drinking water, however, US EPA [75] suggested less than 1000 μS/cm, while the WHO [75] suggested 2500 μS/cm, as the allowable limit of EC in drinking water. NSDWQ [76] affirmed that EC has no deleterious effects on human health. However, a high level of EC in water increases the ionic load and corrosive nature of the water. As shown in Fig. 2e, the elevated EC contents in the borehole water samples could be ascribed to the presence of inorganic solids such as Cl− and SO_4^{2-}, which carries high negatively charged ions, or the presence of Ca^{2+}, Na^{+}, K+, and Mg^{2+} (ions that carry positive charges) [77]. The BOD and COD values of the groundwater were lower than the WHO limits of 5 and < 200 mg/l, respectively. This signifies low levels of organic matters, and low counts of microbes, making the water safe for consumption [78].

The mean concentrations of the hydrogeochemical parameters (cations and anions) are as follows: $HCO_3^- > Ca^{2+} > Na^+ > NO_3^- > Cl^- > SO_4^{2-} > Mg^{2+}$ and K^+ (boreholes), and $HCO_3^- > Cl^- > SO_4^{2-} > Na^+ > NO_3^- > Ca^{2+} > K^+$ and $> Mg^{2+}$ in well water samples. The Na^+ concentrations ranged from 36.87 to 96.49 (mg/l), with a mean value of 65.53 mg/l, which are considerably lower than the 200 mg/l allowable limit recommended by the WHO [71] in drinking. Na+ is considered a dominant cation and its high concentrations in groundwater aquifers has been linked to Na^+ rock weathering or halite dissolution, agrochemical deposits, and salt intrusion through erosion [9]. As halite deposit is lower in the investigated groundwater, it could be said that cation exchange processes are the major factors controlling the hydrogeochemistry of the groundwater in alluvial plain [48]. The Mg^{2+} concentrations ranged between 11.09 and 16.87 (mg/l), with a mean value of 13.28 mg/l, which were within the 50 mg/l limit of the WHO [71]. The predominance of calcium ions in groundwater could be attributed to exchange processes (cations) and the dissolution of carbonate rocks [38]. The Ca^{2+} concentrations ranged from 47.65 to 58.88 (mg/l), with an average value of 51.81 mg/l, although lower than the desirable limit of 75 mg/l considered safe by the WHO [71] in drinking water. The higher concentrations of Ca^{2+} than Mg^{2+} suggests slight dissolution of carbonate materials. Given the absence of calcite and dolomite in the study region, the presence of Ca^{2+} and Mg^{2+} in the aquifer groundwater could be due to chemical fragmentation of silicate particles such as pyroxenes and calcilagioclase feldspars [79]. The concentrations of K^+ in all the examined groundwaters were below the 12 mg/l suggested by WHO.

In reference to the anions, SO_4^{2-} levels ranged from 19.94 to 53.67 mg/l, with a mean of 35.13 mg/l, which were within the permissible limits of 400 mg/l (Table 2). The distribution patterns of SO_4^{2-} were heterogenous, with higher concentrations observed in the hand-dug wells compared to the borehole water samples (Fig. 2l). This could be due to the differences in the designs of both water sources, given that well water, due to its open structure, wider, greater depth, and surface area, tends to be more susceptible to geological processes (gypsum or anhydrite mineral weathering), and anthropogenic activities (leaching of agricultural fertilizers, household wastes, and the percolation of leachate plumbs from nearby landfills and municipal sewage systems) that are being intensified within the study region. Conversely, Cl^- showed homogeneous distribution pattern and the levels ranged from 20.43 to 27.16 mg/l, which were within the maximum allowable limits of 250 mg/l (Table 2) for drinking water. Elevated levels of SO_4^{2-} and Cl− are mostly observed in groundwater within the discharge region [67], however, the low concentrations denote that the sampled groundwater might be located in the regional recharge point of the study area. NO_3^- is generally observed in groundwater at low concentrations, but it can increase as a result of runoff or even human interference, such as leaching fertilizers used for farming purposes or human and even animal waste. In this study, the NO_3^-levels ranged from 32.65 to 44.25 mg/l (borehole) and 15.15–18.45 mg/l (well), and were much below the 50 mg/l suggested by the WHO [71]. The concentrations of HCO_3^- ranged from 64.13 to 95.07

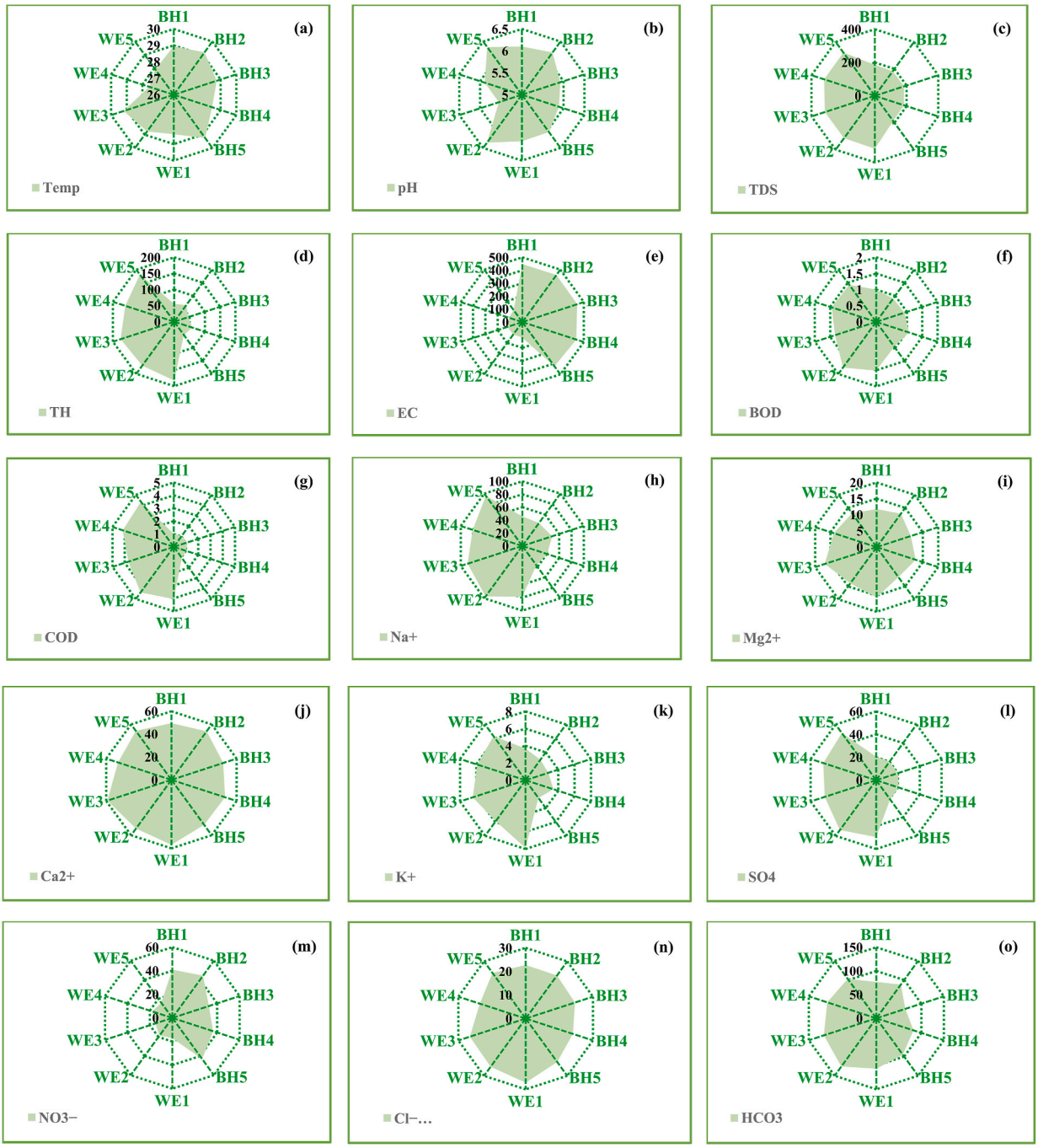

Fig. 2. (a–o): Distribution trends of physicochemical and hydrogeochemical parameters in boreholes and hand-dug wells.

(mg/l) in boreholes and 102.70–125.82 (mg/l) in well groundwaters, which were below the allowable range of 250 mg/l. The relatively similar, yet low levels of HCO_3^- in all the examined groundwaters demonstrate that decaying organic matter has little or no influence on the dissolution processes of minerals in the aquifer [34].

4.2. *Spatial distribution of hydrogeochemical ions in groundwater*

The spatial distributions of physicochemical and hydrogeochemical parameters in ten groundwater samples in Ojo region were evaluated (Fig. 3). The northeast, northwest, southeast, and southwest quadrants of the study area were the locations of the analyzed groundwater. The findings showed different contamination levels and characteristics, impacted by environmental factors, human-

induced activities, and geological processes. As shown in Fig. 3a, the pH levels of groundwater samples across all regions were found to be slightly acidic (below 7). The pH of groundwater was largely influenced by the geological makeup of the study area, which is made up of sedimentary layers of sandstone, silt, and clay. Yusuf et al. [38] affirmed that due to the leaching of organic acids and cations from the topsoil, clayey deposits may increase acidity. The slightly acidic pH of the groundwater could also be a sign of fertilizer runoff from agriculture, which could lower pH levels [80]. The lowest pH values were found geographically in the northeast and southwest, which may be related to increased industrial discharges and agricultural activity in these areas. Increased nutrient loading from agricultural practices near groundwater sources can impact pH and overall water quality [80]. As a result, the pH distribution across space points to a potential relationship between natural geological processes and human activities. As shown in Fig. 3b, the TDS levels in all the groundwater samples were found to be spatially low to moderate, which could be attributed to the permeable nature of sandy alluvial deposits and the limited retention of dissolved solids in groundwater [81]. The low TDS levels implied that barring over-extraction, saline intrusion—which is frequently a challenge in coastal areas like Ojo—does not substantially affect the groundwater. The moderate TDS levels in some locations, however, might draw attention to specific human influences, like the effluent discharge from adjacent industrial facilities, which can raise dissolved solids through several contaminants.

The spatial analysis showed that hand-dug well waters in the northwest region had higher levels of hardness, but borehole samples

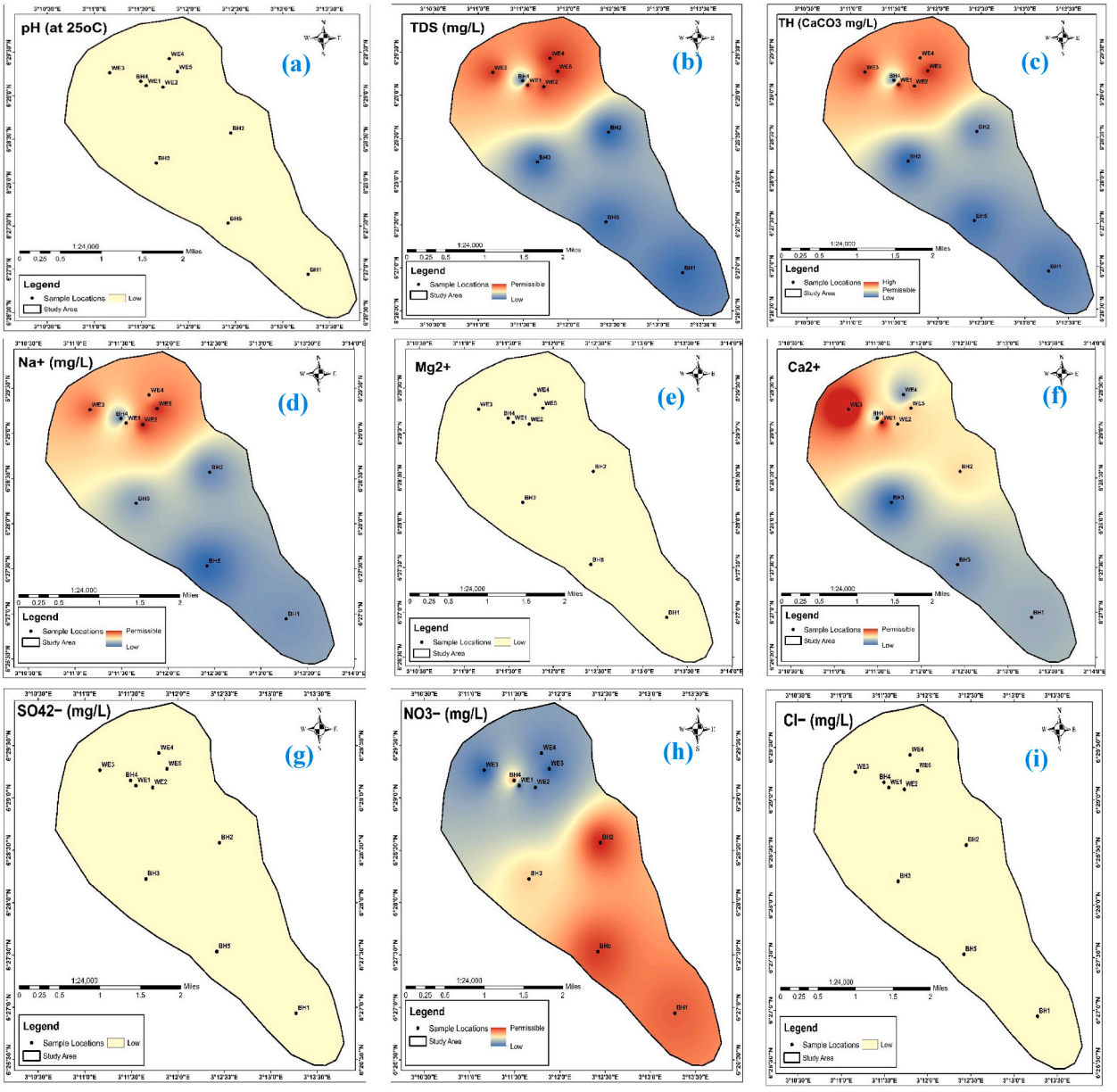

Fig. 3. (a–i): Spatial maps showing the geographical distribution patterns of physicochemical and hydrogeochemical parameters in groundwater.

in the southern (BH1-BH3, BH5) and Northwestern (BH4) regions had low concentrations (Fig. 3b). The variations could be due to differences in anthropogenic inputs and geological processes. Zango et al. [82] reported that boreholes are commonly used to access deeper groundwater sources that are less affected by surface runoff and human activity. Hand-dug wells, on the other hand, are mostly used for accessing shallow aquifers that are more vulnerable to surface forces, such as industrial discharge and agricultural runoff [83]. The leaching of minerals from fertilizers and other agrochemicals into the aquifer groundwater may be the cause of the elevated hardness levels in the Northwestern region, which could be attributed to the agricultural activities in this location.

The concentrations of Na+ in all groundwater samples were found to be moderate (Fig. 3d), whcih suggest that anthropogenic inputs or saline intrusion from nearby coast had low impacts on cation. Given that some fertilizers have the ability to introduce Na+ into groundwater, the spatial distribution of Na+ points to a possible connection with agricultural practices [84]. The moderate effects of nearby seawater on the Na+ levels suggest that the natural hydrological features of the aquifer in the study region prevented large saline intrusion, thus encouraging good groundwater flow [85]. The concentrations of Mg^{2+} (Fig. 3e) and Ca^{2+} (Fig. 3f) were found to be low to moderate in all regions, which is consistent with the local geological profile. Generally, the mineral content of groundwater is influenced by deposits of clay, sand, and gravel; less permeable layers act as barriers to the movement of these ions [41]. Mg^{2+} and Ca^{2+} concentrations did not significantly differ spatially among the sampled groundwaters, indicating a relatively uniform mineral composition. This consistency might suggest that local precipitation serves as Ojo's main source of groundwater replenishment, limiting the entry of outside pollutants and fostering stable mineral levels [40].

The investigated groundwater had low concentrations of SO_4^{2-} (Fig. 3g), NO_3- (Fig. 3h), and Cl- (Fig. 3i), with some variations between samples taken from boreholes and wells. These discoveries are important for comprehending how human activities and natural processes have impacted the study region. The geological makeup of the study area, where the sedimentary layers primarily consist of alluvial sand and clay deposits that contributes little to SO_4^2 concentrations [86]. This explains the low levels of SO_4^{2-} found in all the regions. This might be due absence of nearby industries that frequently release SO_4^{2-} compounds. The consistency of SO_4^{2-} concentrations suggest that the groundwater in Ojo region is comparatively safe to drink because it is not as affected by pollution sources. It does, however, bring up concerns about the possibility that, if not adequately managed, future industrial developments, like the Volkswagen assembly plant or other nearby manufacturing facilities, could introduce SO_4^{2-} and other contaminants into the groundwater system. In well water samples, NO_3 concentrations were found to be significantly higher than in borehole samples. The vulnerability of shallow aquifers to surface contamination from agricultural runoff, which frequently contains nitrogenous fertilizers, can be used to explain this discrepancy [83]. The spatial distribution shows higher nitrate levels in the northwest, where agricultural practices are more common (Fig. 3h). This demonstrates that fertilizer-treated field runoff contaminates groundwater and could be detrimental to human health if concentrations exceed the prescribed limits [87]. Comparably, Cl-concentrations were discovered to be low to moderate in the sampled groundwaters, indicating that there was little to no interaction between seawater and the aquifer system of the study area. It is possible that hydraulic gradients and local geology have a significant impact on the dynamics of groundwater flow. In addition, the presence of sandy alluvial deposits promotes lateral groundwater movement and recharge, which lessens the impact of saltwater intrusion from the adjacent Atlantic Ocean and lagoon systems [88].

4.3. Assessment of groundwater hydrogeochemistry

4.3.1. Hydrogeochemical distributions

Fig. 4 illustrates a Schoeller plot that graphically depicts the concentrations (meq/l) of the eight (8) hydrogeochemical ions identified in the groundwater. This plot explains the ion exchange and mobility processes between hydrogeochemical variables in aquifer system [52]. The hydrogeochemistry of the aquifer in the Ojo region is primarily characterized/dominated by the prevalence of Na^+, Ca^{2+}, and HCO_3^-. The distribution patterns of chemical ions are in this order: $Na^+ > Ca^{2+} > HCO_3^- > Mg^{2+} > SO_4^{2-} > Cl^- > NO_3^- >$

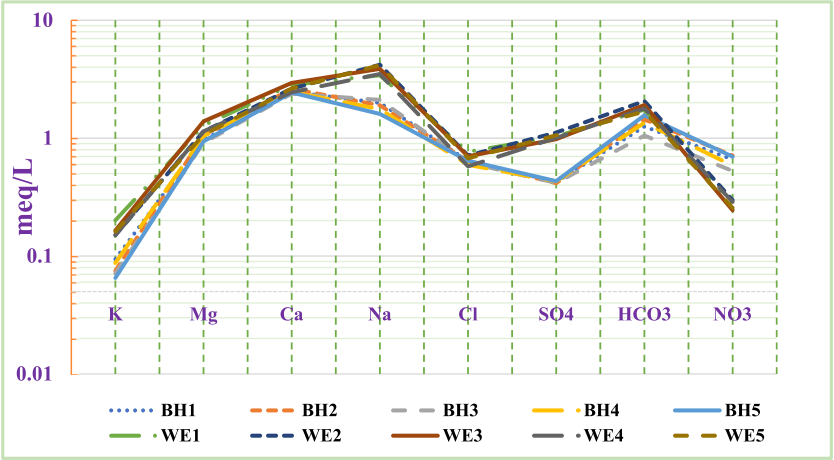

Fig. 4. Schoeller diagram showing the distributions of the chemical ions in groundwater.

and K^+. Elevated concentrations of Na^+ demonstrate the dissolution of numerous kinds of rocks that form aluminum tectosilicate or alkali minerals, while high levels of Ca^{2+} suggests the dissolution of minerals containing Ca ions in the aquifer system [23]. The elevated concentrations of HCO_3^- compared with SO_4^{2-} implies that the dissolution of carbonic acids, geological weathering of silicate rocks, and other minerals are more dominant than sulfide oxidization processes in the aquifer, thus influencing the geochemical attributes of groundwater sources. Nonetheless, the HCO_3^- levels were significantly below the permissible limits and, as a result, were not enough to influence or increase the pH of the groundwater. At low Na^+ and Cl^- concentrations—extremely below the recommended limits—it could be inferred that the influence of seawater intrusion processes or dissolving salts from evaporite deposits are minimal in the study region [89]. NO_3^- and K^+ had the lowest concentrations and were below the allowable limits in drinking water. This clearly indicates that K–felspar geological material in aquifer was resilient to chemical dissolution. It has been reported that the inability of NO_3^- to contaminate groundwater systems could be due to excessive rainfall, which results in chemical dilution, or the excessive availability of green–healthy plants, including trees and vegetation, which tend to trigger denitrification processes [23]. Similarly, low Mg2+ levels in this study indicate insufficient CO2 in the groundwater system and inadequate ferromagnesian and dolomite mineral decomposition processes.

4.3.2. *Hydrogeochemical facies and water types*

The geological structure and the hydrological and geochemical processes within an aquifer system are considered the most important factors influencing the cation and anion variables in groundwater. Thus, assessing the hydrogeochemical facies is essential for comprehending and identifying the geological and geochemical factors influencing the regional flow pattern and hydrogeochemical characteristics of groundwater [90]. This study used the conventional Piper trilinear diagram to characterize the hyrogeochemical ions in order to clearly understand the water types and hydrogeochemical facies of the aquifer groundwater in the Ojo district. Fig. 5 is the piper diagram showing the triangular cation and anion domains (measured in milliequivalent concentrations) projected into the multidimensional diamond at the center. It was observed that over 80 % of the cations were distributed in the "no dominant type" zone, except for a few samples in which Na^+ and Mg^+ were strongly influential. Conversely, the anion triangle revealed that most of the anions were strongly dominated by HCO_3^- (weak acids), with only three (3) groundwater samples showing partial inclinations in the non-dominant type zone. The presence of unsaturated precipitation, filtration, or atmospheric dissolution of some compounds of gases and minerals, particularly CO_2 and CO_3, within the study area could be responsible for the dominant nature of the HCO_3^- water type [91]. The low variations observed in the distributions of chemical ions (cations and anions) demonstrate similarities in chemical properties and geochemical activities. The diamond shape revealed that the groundwater geochemistry is characterized by three types of water. Ca^{2+}–Mg^+–HCO_3^- (alkaline earth–bicarbonate) is the most dominant, accounting for 65 % of the total hydrogeochemical facies. This outcome supported the notion that the study area is located within the radius of some lagoons (Lagos Lagoon Complex and Ologe Lagoon) that are enriched in Ca^{2+} and HCO_3^- and, as a result, recharge directly from these Lagoon systems. The mixing zone accounts for just 30 %, indicating a "low to moderate" salinity influence and shallow–plain groundwater facies. Na^+–K^+–Cl^-–HCO_3^- accounted for 5 % of the hydrogeochemical facies, inferring minimal seawater intrusion or salt dissolution influence on the Na^+ and Cl^- compositions of the groundwater, which corroborates the outcome of the Schoeller plots reported earlier.

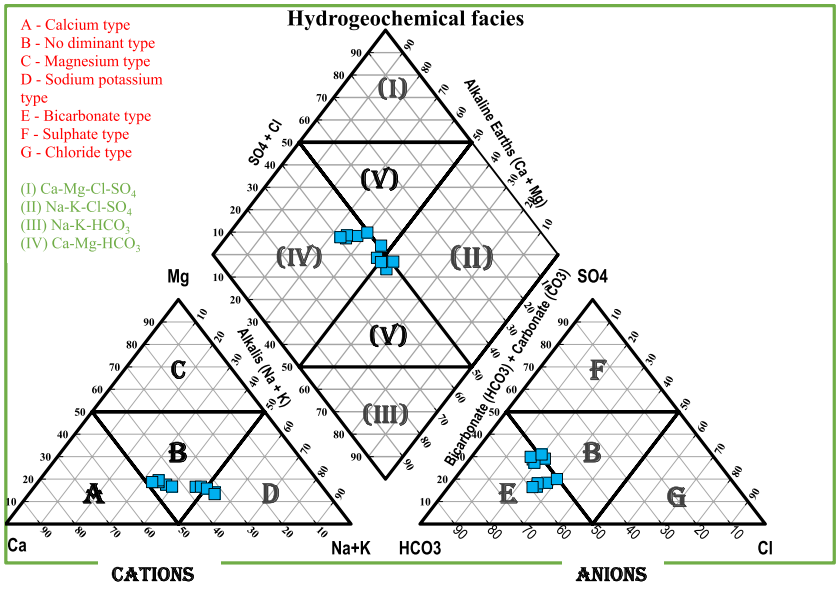

Fig. 5. Piper trilinear diagram showing the water type and hydrogeochemical facies of groundwater.

4.3.3. Hydrogeochemical processes (interionic ratios and subsurface mechanisms)

4.3.3.1. Weathering and dissolution. The hydrogeochemical attributes of an aquifer system are influenced by numerous ion exchange mechanisms and processes that could generally impact the quality of groundwater (Li et al., 2013). The interionic ratios and geochemical interactions between the chemical ions (Na^+ versus Cl^-; $Na^+ + K^+$ versus Cl^-; $Ca^{2+} + Mg^{2+}$ versus $HCO_3^- + SO_4^{2-}$; SO_4^{2-} vs Ca^{2+}; $Ca^{2+} + Mg^{2+} - HCO_3^- - SO_4^{2-}$ versus $Na^+ - Cl^-$; Cl^-/HCO_3^- versus Cl^-; HCO_3^-/Na^+ versus Ca^{2+}/Na^+ and Mg^{2+}/Na^+ versus Ca^{2+}/Na^+) in this study are represented in figures (6a–6h) below to ascertain the origin and chemical constituents of groundwater in the study area.

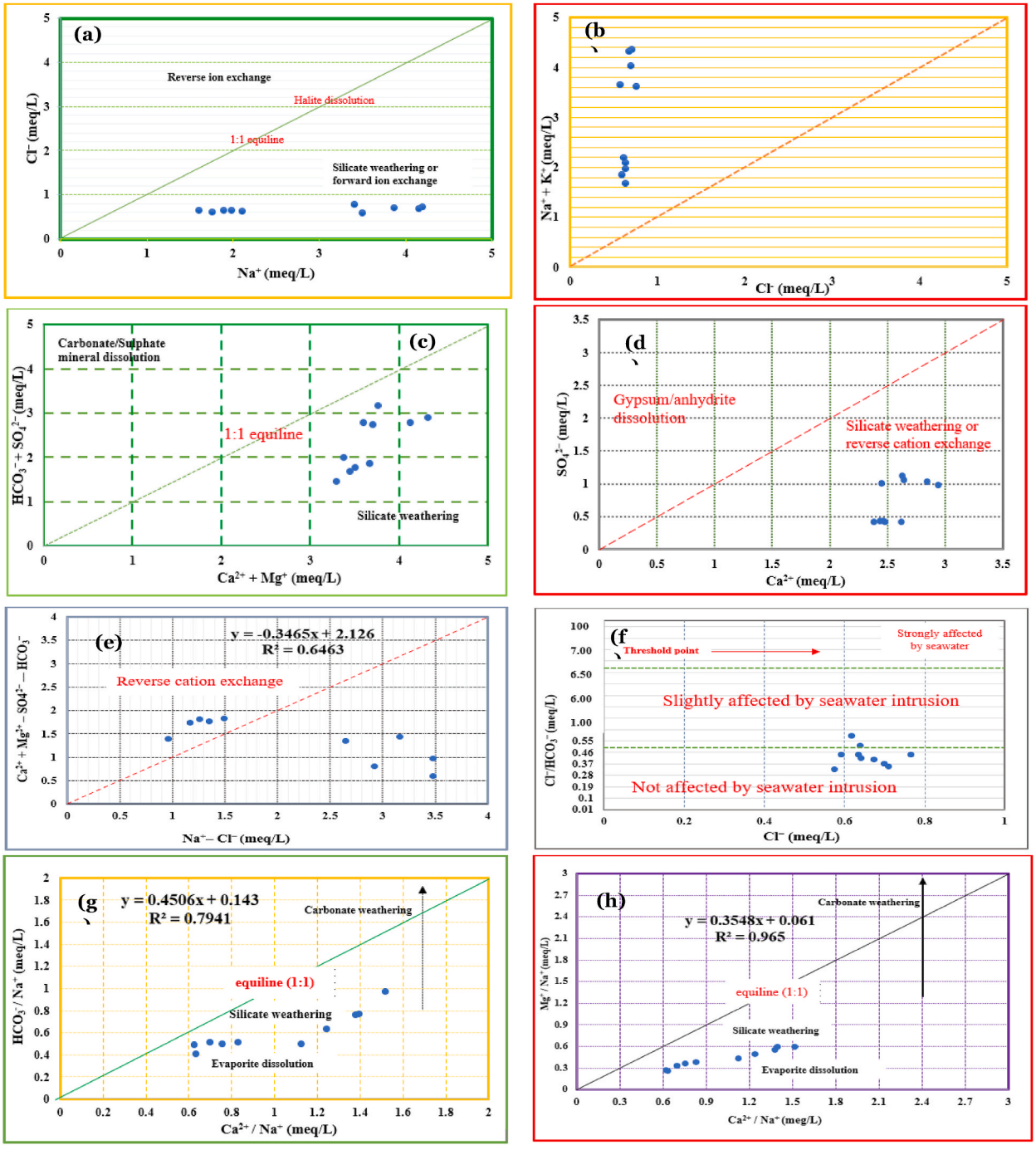

Fig. 6. (a–h): Scatter plots indicating stoichiometric relationships between various hydrogeochemical ions in groundwater.

Fig. 6a illustrates the linear correlation observed between Na^+ and Cl^-. Basically, mineral dissolution is responsible for the high Na^+ and Cl^- concentrations in groundwater. These ions are shown in the plot graph to be within the equiline level (1:1), which indicates that halite dissolution was the source of these ions [32]. The groundwater samples in this present study fell substantially below the equiline (1:1) due to the high Na^+ level compared to the Cl^-. This implies that forward ion exchange is the predominant process, and silicate weathering is the primary geochemical source of Na + [33,92,93]. The higher concentrations of Na^+ compared to Cl^- in groundwater samples may also result from human activity and additional Na + introduction via ionic exchange processes. Fig. 6b shows the ionic exchange processes of Cl− and $Na^+ + K^+$. It was observed that 100 % of the samples were above the equiline (1:1), signifying the presence of excessive cations. This could be a result of the extensive formation of alkali, alkali carbonates, or sulfates in the region. This result is similar to that obtained from the Piper trilinear plot.

The scatter plot of $HCO_3^- + SO_4^{2-}$ vs. $Ca^{2+} + Mg^{2+}$ is illustrated in Fig. 6c. It is evident that an ionic exchange process occurs between chemical ions when the sample plot is moved to the left (reverse ion exchange) or right (forward ion exchange) of the equiline. Furthermore, samples with an ionic ratio above the equiline demonstrate that gypsum, calcite, and dolomite are all dissolved in the aquifer system, while a ratio below 1:1 indicates silicate weathering or precipitation sources. It was observed in this study that all the samples fell downward on the right side, below the equiline. This confirmed the involvement of the ionic exchange process in the chemical hydrology of the examined aquifer groundwater as a result of predominating silicate dissolution rather than carbonate mineral weathering [92,93]. The hydrogeochemical interactions between SO_4^{2-} and Ca^{2+} illustrated in the scatter plot (Fig. 6d) showed that all the samples fell within the range of 1:2. This further confirmed that silicate and not anhydrite or gypsum weathering is the predominant process influencing the hydrogeochemical ions in the aquifer groundwater. Moreover, the low concentrations of all the silicate ions (Cl^-—SO_4^{2-}—HCO_3^-—NO_3^-) further confirmed the anoxic hydrological and geological status of the study area.

The interionic exchange process was further illustrated by plotting $Ca^{2+} + Mg^{2+} - SO4^{2-} - HCO_3^-$ versus $Na^+ - Cl^-$ (Fig. 6e). In a situation where the ion exchange reaction between Cl^- and Na^+ ions clusters toward the zero point on the x ($Na^+ - Cl^-$) axis, subtracting the former from the latter best explains that the speciation of Cl^- is primarily due to precipitation and is an indication that the ionic exchange processes have no effect on the groundwater. Similarly, a value of zero after subtracting $SO4^{2-}$ and HCO_3^- from Ca^{2+}

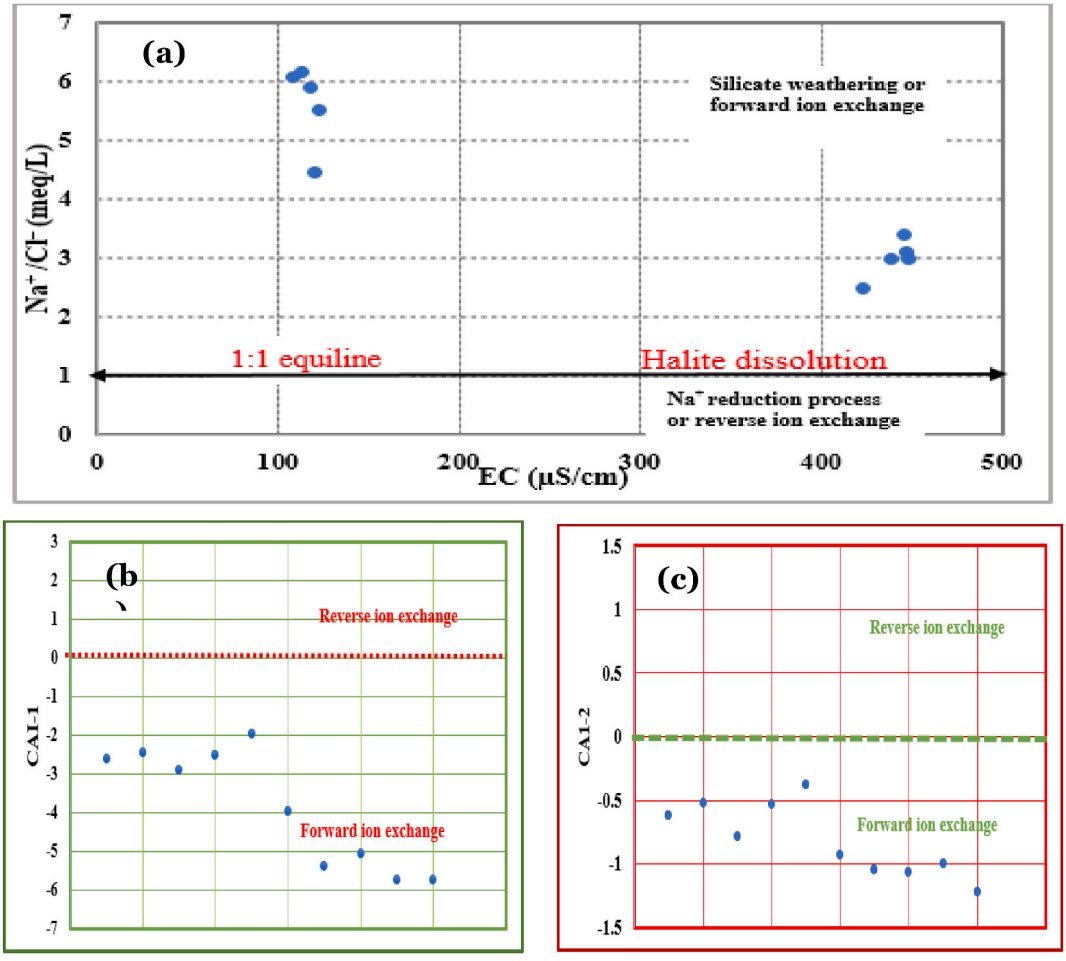

Fig. 7. (a–c): Bivariate plots showing the evaporation and ionic exchange reactions in groundwater.

and Mg^{2+} is an indication of gypsum and dolomite, weathering without the ionic exchange effect [94]. Conversely, an equiline (1:1) slope suggests that the dominant process influencing groundwater is ionic exchange. None of the samples projected toward the zero axis, indicating a great influence of the ionic exchange process on the hydrogeochemical characteristics of the groundwater in the study location. In addition, this plot (Fig. 6e) was used to decipher the significance, involvement, and influence of cation exchange on groundwater hydrochemistry in relation to the aquifer system. The samples would form a line with a −1 slope, provided that the system's most important process is cation exchange. A negative slope of −1 or close to −1 implies substantial involvement of the cation exchange process. This implies that the absorbed ions on the top layer of the pulverized particulates in the aquifers have been replaced with ions in the solutions [95]. Fig. 6e also shows that the groundwater clusters had a negative slope of −0.347 and a correlation coefficient value of 0.646. This implies that cation exchange was insignificant in relation to the concentrations of Mg^{+}, Ca^{2+}, and Na^{+}. This is supported by the presence of only 50 % of the groundwater samples within the reverse cation exchange plot.

Fig. 6f illustrates the molar ratio of Cl^{-} versus Cl^{-}/HCO_3^{-}. The diagram is an essential indicator that measures the rate and impact of seawater intrusion (the salinization effect), identifies water types as well as the sources of the saline contents in the groundwater system. Naidu et al. [34] reported that a molar ratio less than 0.5 implies no saline intrusion effect, a ratio between 0.5 and 6.6 implies a slight to moderate impact of seawater intrusion, while a ratio greater than 6.6 indicates high seawater intrusion, indicating an extreme salinization influence on groundwater. As shown in Figs. 6f, 20 % of the samples fell within the range of slight to moderate seawater effects, while the remaining 80 % were not affected by seawater intrusion. This result aligns with the outcomes of the Schoeller and Piper plots based on seawater intrusion.

The specific effects of rock weathering on the geochemistry of groundwater in relation to carbonate, silicate and evaporite mineral dissolution were examined through Na–normalized molar ratios. Bidimensional diagrams were plotted to depict the molar ratio of HCO_3^{-}/Na^{+} versus Ca^{2+}/Na^{+} (Fig. 6g) and of Mg^{+}/Na^{+} versus Ca^{2+}/Na^{+} (Fig. 6h). A molar ratio above the equiline (1:1) indicates carbonate weathering while the ratio below the equiline demonstrates that the dissolution of silicate minerals influences the ion concentration [9,93]. All the molar ratios of the samples in the plotted diagrams (Fig. g 6and 6h) were found in the left bottom and middle areas, below the equiline (1:1). This finding denotes that both evaporite dissolution and the rock–water interaction of schistose/silicates significantly influenced the hydrogeochemistry of the aquifer system. In addition, the strong regression values obtained from the ion exchange processes between HCO_3^{-}/Na^{+} versus Ca^{2+}/Na^{+} ($r^2 = 0.794$) and Mg^{+}/Na^{+} versus Ca^{2+}/Na^{+} ($r^2 = 0.965$) further confirmed the substantial influence of silicate minerals on the chemical hydrology of the aquifer system in the study region.

4.3.3.2. (ii) evaporation and ion exchange processes. The scatter plot illustrating the reaction between Na^{+}/Cl^{-} vs. EC is represented in Fig. 7a. This plot was used as an indicative element to quantify the influence of evaporation and ionic exchange in aquifer groundwater [92,93]. In this study, the Na^{+}/Cl^{-} molar ratios of all the samples were greater than 1, inclined with the EC concentrations ranging from 10.70 to 448.78 (μS/cm) (less than 1000 μS/cm). This demonstrates that the main process influencing the chemical hydrology of the aquifer groundwater is silicate dissolution, with little evaporation effect (seawater intrusion). Hydrogeochemical ions in groundwater are obtained from the aquiferous particles due to the ionic exchange process in the host environment or during chemical mobility [90]. In an attempt to further comprehend the sources of the chemical ions and the type of ion exchange in the groundwater of this study, the equations CAI–1 = $[Cl^{-} - (Na^{+} + K^{+})/Cl^{-}]$ and CAI–2 = $[Cl^{-} - (Na^{+} + K^{+})/(SO_4^{2-} + HCO_3^{-} + NO_3^{-})]$ were used to calculate the chloro–alkaline indices (Fig. 7b and c). Positive CAI–1 and CAI–2 values indicate ionic exchange reactions between Na+ and Ca2+ [96]. Conversely, negative CAI–1 and CAI–2 values suggest that Ca deposited in the groundwater absorbed the Na substitute. Furthermore, forward and reverse cation exchange are indicated by positive and negative CAI values, respectively. In the present

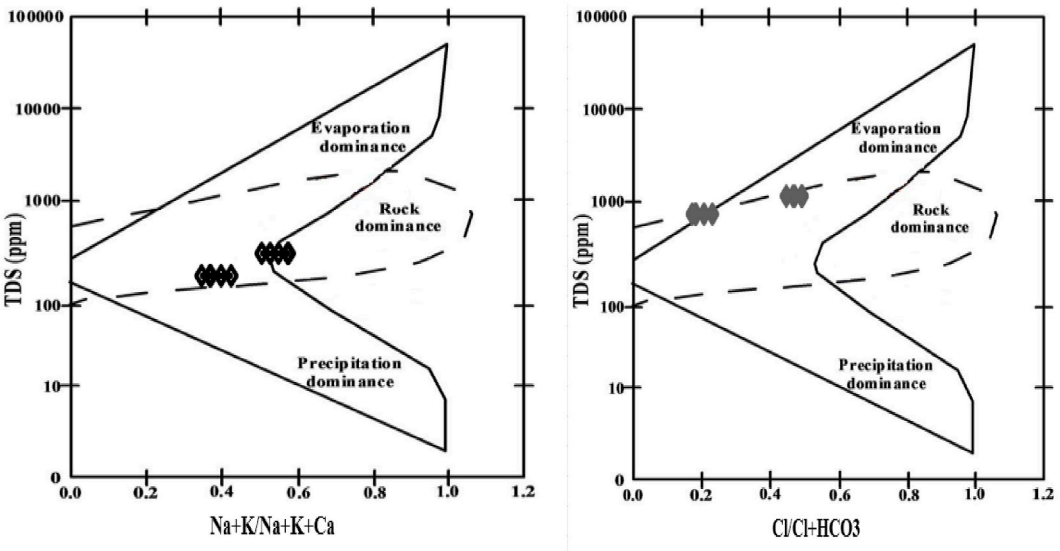

Fig. 8. Gibb's plot illustrating the mechanisms governing chemical ions in an aquifer groundwater system.

study, all of the samples had negative CAI–1 (Fig. 7b) and CAI–2 (Fig. 7c) values. This indicates that forward ion exchange process is primarily responsible for alkali metal (Na + K) released in the examined groundwater.

4.3.4. Mechanisms controlling groundwater chemical hydrology

Gibb's diagram is a hydrogeochemical index that is widely used for deducing the mechanisms that control the processes associated with the sources of chemical ions in groundwater [97]. This source has been widely divided into three (3) layers, namely, precipitation dominance in the lower layer, rock dominance in the midpoint, and evaporation precipitation in the upper layer (Fig. 8). Several researchers have reported that the chemistry of groundwater can be substantially influenced and regulated by numerous hydrological, lithological, and geochemical processes, such as climate events, interactions between rocks and water in relation to the weathering or dissolution of minerals, precipitation, ionic exchange, and anthropogenic activities [52,98]. The ratios of $Na^+/(Na^+ + Ca^{2+})$ and $Cl^-/(Cl^- + HCO_3^-)$ provided in Fig. 8 serves as a function of TDS. In this study, rock dominated the ratios of $Na+/(Na^+ + Ca^{2+})$ to TDS. The ratio of $Cl^-/(Cl^- + HCO_3^-)$ against TDS revealed rock dominance as well as minimum evaporation and precipitation effects in the study area. This result corresponds with the outcome obtained during the ionic exchange process assessment. This demonstrates that the interaction between water and rock in relation to the chemical weathering of mineral rocks had a significant influence on groundwater enrichment. Iqbal et al. [9] mentioned that the dissolution of parent rocks is influenced by the mixing processes of minerals and dissolvable salts in groundwater. The results of this study are comparable to the findings of Yusuf et al. [38] in Lagos along a coastal belt in Nigeria, where rock–water interactions dominated. This finding lends credence to the fact that the groundwater samples were collected in the layer (see hydrogeological description of the study area), where hydrological processes such as deep percolation or groundwater recharge influence groundwater chemistry. The effect of evaporation on the aquifer agreed with the assertion of Edwards et al. [99] that the flat or low–plain nature of a specific region has the tendency to hold water at the top layer for a considerable period before infiltration, which would eventually enhance the evaporation process. It could therefore be inferred that the lithology of the study area, seawater intrusion, and bedrock mineralogy are responsible for the hydrogeochemical formation and condition of aquifergroundwater in Ojo region.

4.4. Heavy metal concentrations in groundwater

Table 3 and Fig. 9 present the summary of nine heavy metals in groundwater from the Ojo district and the standard limits recommended by the WHO. The heavy metal concentrations in the groundwater samples were in the following order: Fe > Mn > Ni > Zn > Pb > As > Cd > Cr > Cu. Basically, As is regarded as a very harmful element, regardless of its concentration. Stomach cramps and

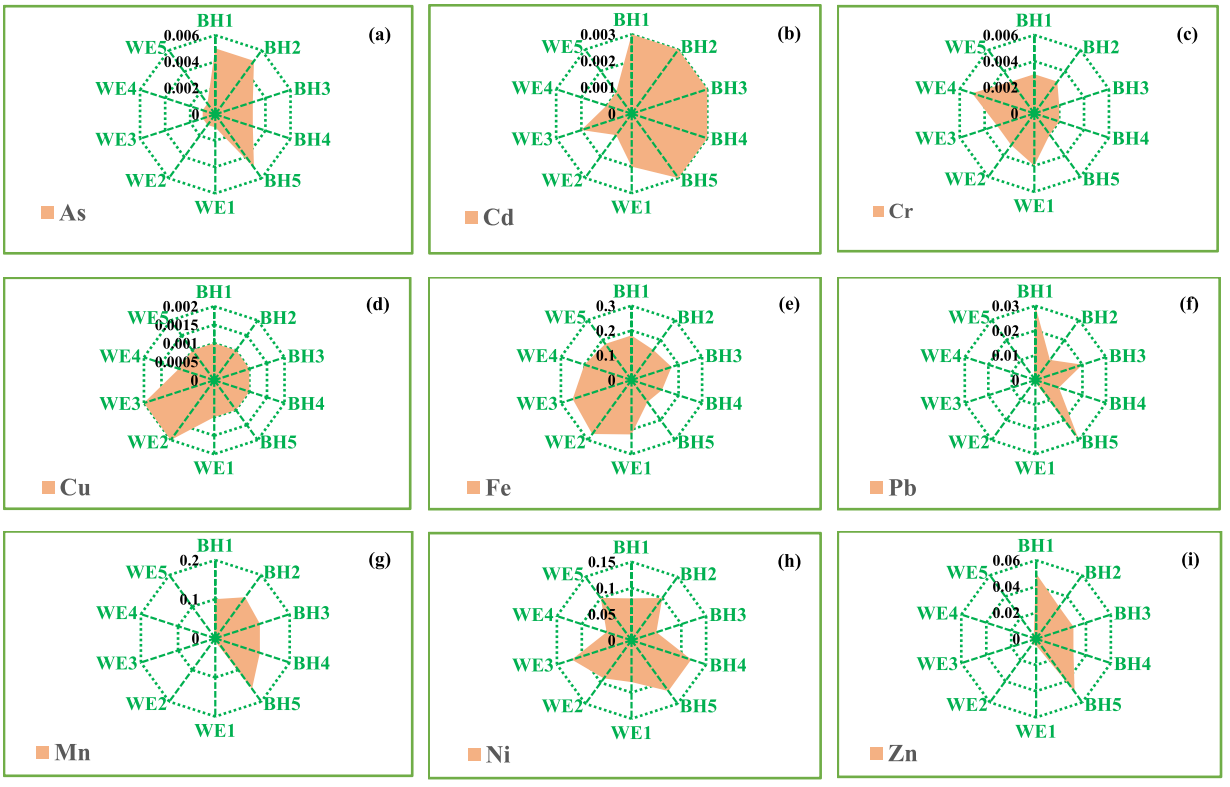

Fig. 9. (a–i): Distribution trends of heavy metals in boreholes and hand-dug wells.

stooling are among the aftereffects linked to exposure to As, especially via ingestion [100]. In the present study, As concentrations ranged from 0.001 to 0.005 mg/l, with a mean of 0.002 mg/l, and were within the maximum allowable limit of 0.010 mg/l recommended by the WHO [71]. The Cd concentrations were homogenously distributed, ranging from 0.001 to 0.003 (mg/l), with a mean of 0.002 mg/l. Essentially, Cr is a trace element that is occasionally detected in both surface water and groundwater systems. The major source of Cr in waterways is the leaching of surface soil as well as improper landfill disposal [101,102]. Obasi and Akudinobi [103] affirmed that Cr is a carcinogenic element, while Chika and Prince [102] confirmed that drinking water with Cr levels above the established limits can cause allergic dermatitis in humans. The Cr levels ranged between 0.002 and 0.005 mg/l, with an average value of 0.003 mg/l. The Cr and Cd in all the groundwater (Fig. 9b and c) fell within the standard limits of the WHO [75] provided in Table 3. Udousoro and Austin [104] reported a similar Cd level in groundwater in River State, Nigeria. The concentrations of Cr were within their respective background values, which points to the geological source of origin [35].

Cu was homogenously distributed in all the groundwater samples (Fig. 9d), and were lower than the 1.5 mg/l allowable limit of WHO [75]. The Fe contents ranged from 0.11 to 0.27 mg/l and were below the standard limits of the WHO (Table 3). The Pb levels ranged between 0.001 and 0.003 mg/l, with a mean of 0.186 mg/l. As shown in Fig. 9f, the Pb concentrations in boreholes were higher than those in well water, with some samples [BH1 (0.03 mg/l), BH3 (0.02 mg/l), and BH5 (0.03 mg/l)] exceeding the standard limits considered safe for drinking. The elevated Pb levels of the groundwaters could be traced directly to the industrial leaching of steel produced by the Volkswagen assembly facilities or discharge from other local industries within the study. In addition, Gibson et al. [105] reported that the rusting of galvanized materials is accelerated during borehole setup when lead pipes are secured with copper lines using brass fittings. This leads to higher Pb concentrations in the borehole water supply. Pb poisoning in children can result in weight loss and convulsions and can also affect the reproductive system, increase cholesterol levels, induce joint and muscular pain, and cause problems with cognition or focus in adults [106,107]. In addition, Pb slows the mental health of newborns and is hazardous to the central and peripheral nervous systems [102].

The concentrations of Mn in the examined groundwater samples ranged between 0.003 and 0.16 (mg/l), with a mean value of 0.066 mg/l. Fig. 9g revealed that Mn levels in all the borehole water samples were higher than the allowable limit of 0.08 mg/l considered safe in drinking water [75]. The high levels of Mn recorded in the borehole water samples could be attributed to local discharge from the Volkswagen steel facilities, given that this industry is located closely to the area where the examined boreholes were erected (Fig. 1). Leaded gasoline, household waste, and plumbing materials have also been linked to high Mn levels in water [108]. The prolonged consumption of water with incredibly high Mn concentrations could result in the previously mentioned adverse effects on humans. Both humans and animals need Ni in their diets, but too much Ni can be toxic and consequently cause cancer, particularly in women [109]. The Ni concentrations varied from 0.05 to 0.12 mg/l, with a mean value of 0.091 mg/l. As provided in Fig. 9h, over 60 % of the groundwater samples had Ni contents which exceeded the 0.07 mg/l (Table 3) maximum permissible limit considered safe in drinking water. Ni levels in groundwater were high as a result of extensive geological weathering of Ni ore-bearing rocks and soils [36]. Similarly, it could be due to local industrial pollution in the study area, as the leaching of rusted steels and

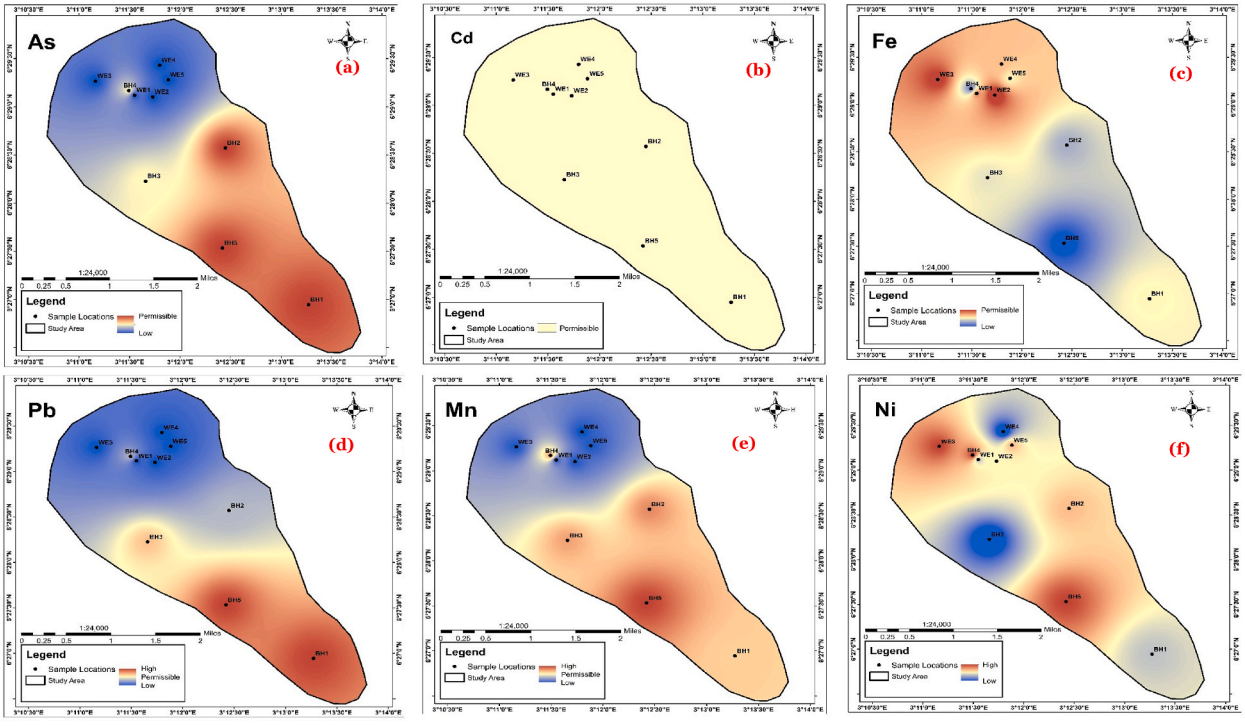

Fig. 10. (a–f): Spatial maps showing the geographical distribution patterns of heavy metals in groundwater.

wastewater discharge can increase Ni concentrations [35]. Conversely, the Zn levels in groundwater were extremely below the standard value (3.00 mg/l) for safe consumption.

4.5. Spatial distribution of heavy metals in groundwater

The spatial distribution patterns of six heavy metals in groundwater based on geographical locations are illustrated in Fig. 10. Significant differences exist between different geographical regions in the spatial distribution of contaminants like As, Pb, Mn, and Ni found in groundwater samples, especially when it comes to hydrological features and proximity to industrial activities. As concentrations were within the acceptable limits in all the groundwater samples (Fig. 10a). Although hand-dug wells in the northern region showed lower concentrations than the borehole water samples near the Volkswagen assembly facility. This geographical pattern of distribution points to a restricted effect of industrial operations on groundwater quality. The groundwater system may be more susceptible to the leaching of As from industrial processes or related waste materials due to the assembly plant's close proximity. Prior studies have demonstrated that industrial operations can increase groundwater arsenic levels [92,93].

All groundwater samples, regardless of their geographical location, exhibited significantly low levels of Cd (Fig. 10b). The consistency of the low concentrations of Cd could be attributed to the inherent geochemical makeup of the Ojo region and the efficiency of the current laws governing the emissions of Cd from industrial sources [110]. These results could also be explained by the lack of notable anthropogenic sources of Cd in the area, which is consistent with research demonstrating the natural attenuation capacity of coastal aquifers [111]. The spatial trend of the Fe content in the groundwater samples was evident in Fig. 10c, where it was found to be lower in boreholes and moderate in hand-dug wells. The shallower depth of hand-dug wells may be the reason for the higher Fe levels found, as it allows for greater interaction with organic matter and surface contaminants [112]. Microbial processes have the potential to mobilize Fe, especially in reducing environments that are frequently found in coastal regions [113]. Lower Fe concentrations in boreholes could also be a sign of longer-residence times in deeper groundwater, allowing natural filtration processes to reduce Fe concentrations [111].

Pb concentrations showed an interestingly unique spatial pattern, with two boreholes in the northeast and north and lower levels in hand-dug wells (Fig. 10d). Conversely, Pb concentrations above allowable limits were found in boreholes close to the Volkswagen steel plants in the southern and southwestern regions. This finding emphasizes how industrial operations affect the quality of groundwater. This might have been influenced by the Pb released from industrial emissions in this region [35,47]. The Mn levels were largely low in all hand-dug wells and one borehole in the northern area, but they were high in the remaining borehole samples close to the Ojo Riverine systems and Volkswagen steel industry (Fig. 10e). Anthropogenic inputs from the surrounding industrial facilities may be responsible for the higher concentrations in these areas. These inputs may increase the mobilization of Mn through runoff or leachate [36]. Given that river water has the ability to introduce dissolved metals into the aquifer, the hydrological relationship between the riverine systems and groundwater may also have an impact on Mn dynamics [114]. With the exception of two hand-dug wells in the northern region and one borehole in the southeast, all groundwater samples had Ni concentrations above allowable limits (Fig. 10f). High concentrations of Ni highlight the pervasive impact of industrial activity, especially the assembly of automobiles and related industrial processes. Ni can seep into groundwater systems, particularly in areas with high permeability. Ni is a common contaminant in industrial wastewater [114]. The localized effects of industrial emissions and runoff may be reflected in the spatial distribution of Ni.

The complex arrangement of sedimentary layers that characterizes the geological profile of the study region is a major factor in the spatial distribution of contaminants found in groundwater. The heterogeneous aquifer system that is created by the coexistence of gravelly strata, clay layers, and sandy alluvial deposits affects the movement of groundwater and the transport of contaminants [38]. Contaminants can move laterally due to the permeable character of sandstone alluvial deposits, which promotes groundwater recharge and flow [111]. Pollutants from industrial areas may be transported into the larger aquifer system through high-permeability zones [111]. On the other hand, clay layers act as confining units, limiting vertical movement and generating pressure differentials that can affect the flow direction of groundwater. Contaminants may also accumulate in localized areas as a result of this stratification, especially in close proximity to sources of pollution like the Volkswagen steel facility. Saline water can move quickly in Ojo due to the presence of gravelly and sandy alluvial deposits, which can further complicate the geochemical dynamics of the aquifer.

Elevated levels of contaminants like Ni and Mn can result from the leaching from the surrounding sediments, facilitated by the intrusion of seawater. Complex ion exchange processes that arise from the interaction of freshwater and saline water may also have an impact on the bioavailability of specific metals and how readily plants and aquatic life absorb them [115]. The possible effects of industrial discharges on groundwater quality are highlighted by the elevated levels of Pb, Mn, and Ni in borehole samples taken close to the Volkswagen plant. Heavy metals are frequently used in industrial processes, and they can enter the groundwater system in a number of ways, such as through atmospheric deposition, runoff, and direct discharge [116].

Additionally, the geological features of the investigated region tend to cause these pollutants to build up in the aquifer, which can pose serious health risks to the local population, especially in areas where groundwater is the main source of drinking water. The groundwater in the Ojo region is contaminated by industrial operations as well as agricultural practices. Hazardous materials may seep into the aquifer as a result of the use of agrochemicals, such as fertilizers and pesticides. Agrochemical contamination of groundwater has been documented on a regular basis, which emphasizes the need for sustainable farming methods that reduce chemical use and encourage natural substitutes [117].

4.6. Indexical assessment for groundwater pollution and quality

4.6.1. Single factor pollution index (Pi)

Fig. 11 presents the Pi values of nine (9) heavy metals in groundwater samples from the Ojo district. This index does not reflect the comprehensive status of water quality but rather estimates the extent to which individual heavy metals contribute to water toxicity [118]. The ranges of Pi values for metals in the groundwater samples were as follows: As (0.3–0.5), Cd (1–1), Cr (0.001–0.001), Cu (0.001–0.001), Fe (0.37–0.60), Pb (1–3.00), Mn (2.00–3.2), Ni (2.5–6.00), and Zn (0.01–0.02) in the borehole water samples, while As (0.1–0.1), Cd (0.33–0.67), Cr (0.06–0.08), Cu (0.001–0.001), Fe (0.60–0.90), Pb (0.1–0.1), Mn (0.06–0.16), Ni (2.5–6.00), and Zn (0.001–0.002) in the well water samples. The Pi values of As, Fe, Cr, Cu, and Zn in all the groundwater samples were lower than 1 ($\leq$1), implying “no contamination." The Pi values of Cr fell in the category of "no–low contamination." Low Pi scores were obtained for Pb except for samples [BH1 (3.00), BH2 (2.00), and BH5 (3.00)] with “moderate–high contamination” levels. Similarly, the Pi of Mn ranges from 2.0 to 3.2 in all the borehole waters, which denotes moderate to extremely high Mn toxicity. Pi scores above 3 (extremely high contamination) were obtained for Ni in 80 % of the groundwater samples except for BH3 and WE4. This indicates that the consumption of groundwater in Ojo District could pose a deleterious risk to adults and children as far as Pb, Mn, and Ni are concerned.

4.6.2. Multi–contamination indices

To determine the overall contributions of heavy metals to groundwater pollution, four pollution metrics (Y_N, C_{degree}, HPI, and MHI) were computed (Table 4). In this study, the Y_N values ranged from 1.453 to 1.521 (borehole) and from 1.287 to 1.416 (well). These values were less than 2, and fell in the classification scale of ($1 \leq Y_N \leq 2.5$), indicating slight groundwater pollution. As observed in Table 4, the C–degree values in the groundwater samples were between −3.758 and 4.224. These values were below 40, implying that all the groundwater samples exhibited a low contamination degree (<40). It has been suggested that an HPI of less than 100 (HPI <100) implies no metal pollution or toxicity [35]. In this study, 100 % of the samples were below 100, which further demonstrates that the groundwater samples are not metal–polluted. The outcome of the MHI also follows the trends of other pollution indices. According to Egbueri & Unigwe [51], the NMI below 50 denotes excellent groundwater quality. In the present study, none of the samples had MHI values above 2, suggesting that these samples are excellent and pollution–free groundwater resources.

4.6.3. Groundwater quality index (GWQI) and water pollution index (WPI)

The GWQI is regarded as an all–inclusive rating system that captures the combined impact of all the water parameters on the overall groundwater quality. This essential index provides a clear reflection of the appropriateness of water for utilization [23]. Table S2 depicts the assigned entropy weightage units (Wi) as well as the relative weightage units (Wu) used to compute the GWQI values. The Wi values were assigned to each water parameter in accordance with their effect on the general quality and contribution to the toxicity degree in groundwater. The computed GWQI values of the groundwater in this study are provided in Fig. 12a. The groundwater samples had the following WQI scores: BH1 (82.99), BH2 (79.60), BH3 (65.52), BH4 (82.39), BH5 (101.22), WE1 (59.39), WE2 (62.93), WE3 (72.73), WE4 (47.02) and WE5 (64.52). Based on the classification grades and ratings provided in Table S3, 10 % (WE4) of the water samples were classified as class B, which is categorized as “clean water”. 50 % of the water samples (BH3, WE1, WE2, WE3, and WE5) are class C, inferring poor or moderately unclean water. 30 % of the water samples (BH1, BH2 and BH4) belongs to class D, which denotes very poor and highly unclean water. The BH5 sample falls in class E, which implies extremely unclean water that should not be consumed except when properly treated. Conclusively, none of the investigated groundwater samples is clean enough to meet the standard purity level (Class A) required for drinking purpose, with the borehole samples the most polluted and unsuitable for human utilization. In reference to the WPI (Fig. 12b), the groundwater samples fell into different categories based on the rating scale provided in Table S3. Nonetheless, 70 % of the groundwaters were in the category of “good water” (WPI = 0.5–0.75), while 30 % were classified as “moderately polluted” groundwater. The outcome of the WPI clearly indicated that the groundwater is neither excellent nor extremely polluted.

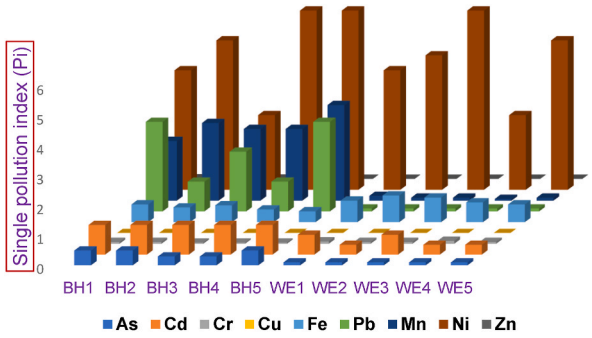

Fig. 11. Single factor pollution of nine (9) heavy metals in groundwater.

Table 4
Pollution indices for comprehensive evaluation of heavy metals in contaminated groundwater.

Indices	Y_N		C_{degree}		HPI		MHI	
Samples	Score	Status	Score	Status	Score	Status	Score	Status
BH1	1.498	Slightly polluted	1.277	Low contamination	56.011	Not pollution	1.317	Excellent
BH2	1.465	Slightly polluted	0.771	Low contamination	27.900	Not pollution	1.236	Excellent
BH3	1.448	Slightly polluted	−1.083	Low contamination	39.143	Not pollution	0.989	Excellent
BH4	1.453	Slightly polluted	1.284	Low contamination	24.211	Not pollution	1.312	Excellent
BH5	1.521	Slightly polluted	4.224	Low contamination	53.231	Not pollution	1.689	Excellent
WE1	1.359	Slightly polluted	−3.758	Low contamination	12.632	Not pollution	0.684	Excellent
WE2	1.402	Slightly polluted	−3.204	Low contamination	13.718	Not pollution	0.756	Excellent
WE3	1.416	Slightly polluted	−1.738	Low contamination	13.448	Not pollution	0.956	Excellent
WE4	1.287	Slightly polluted	−5.438	Low contamination	11.726	Not pollution	0.461	Excellent
WE5	1.328	Slightly polluted	−3.005	Low contamination	10.469	Not pollution	0.791	Excellent

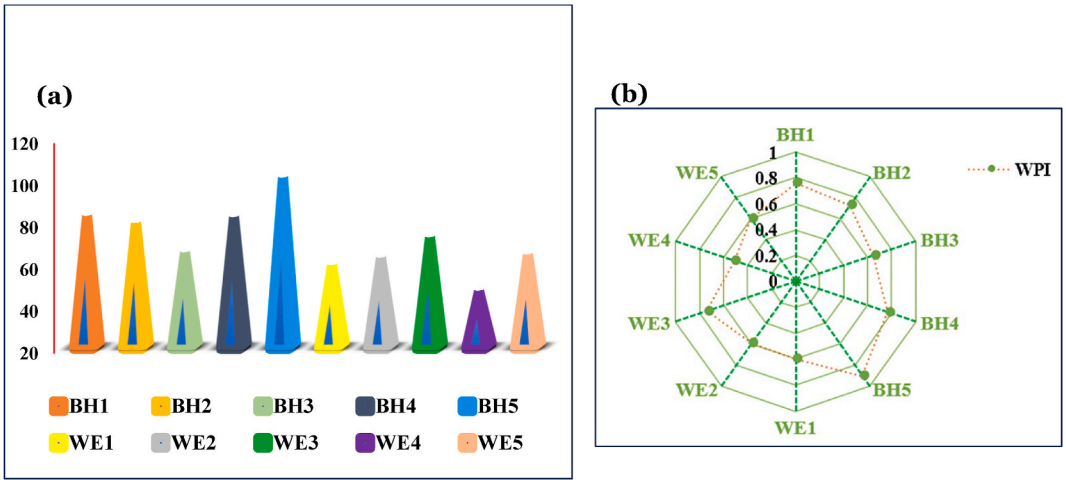

Fig. 12. (a–b): Quality assessment of groundwater (a) Groundwater quality index (b) Water pollution index.

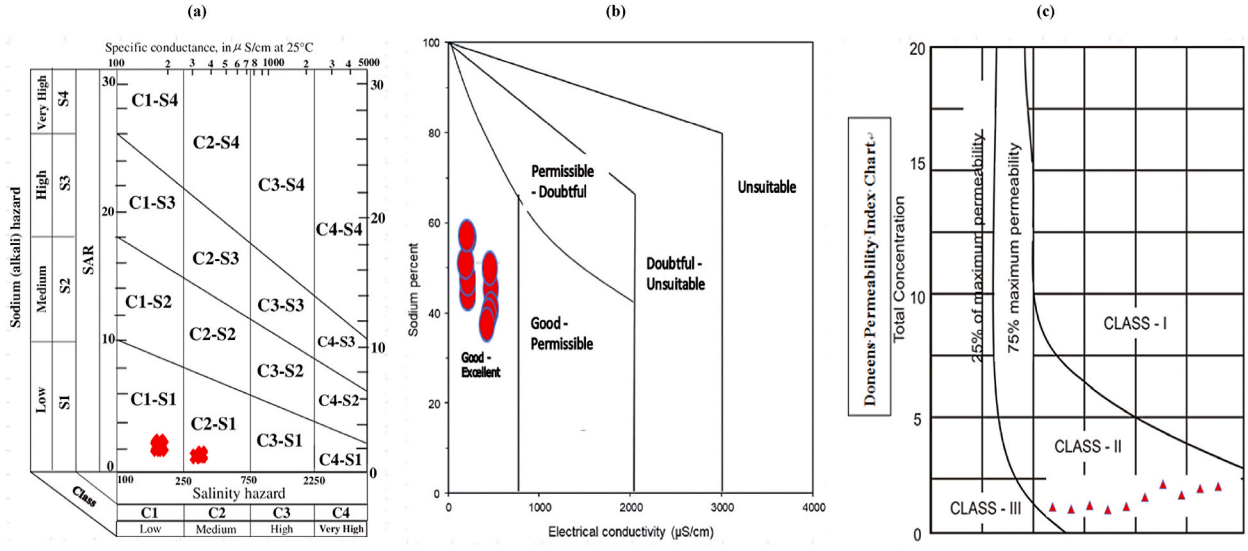

Fig. 13. Suitability assessment of groundwater for irrigation (a) USSL Salinity hazard assessment (b) Wilcox diagram (c) Doneen permeability index.

4.7. Suitability assessment of groundwater for irrigation practices

To determine the suitability of the investigated groundwaters for agricultural practices, five (5) irrigation indices were computed and the results were illustrated in Fig. 13 and Table S6.

4.7.1. sodium absorption ratio (SAR)

SAR is an essential index used for measuring the sodicity status as well as for providing necessary information on the amount of Na absorbed by the soil [119,120]. The amount of irrigation water available to plants is dependent on the ratio of Na, Ca, and Mg in the soil. Wali et al. [121] confirmed that the SAR greater than 10 demonstrates that the absorbed Mg and Ca are displaced by Na, which could substantially impair soil physical properties, thereby limiting the water absorption potential of plants. In this study, the SAR values (Table S6) range between 1.016 and 2.103, implying that all the groundwater samples are excellent for irrigation purposes, based on the ratings provided in Table 1. More specifically, the USSL diagram illustrated in Fig. 13a was used to discern the salinity hazard based on the SAR and EC values. The salinity hazard rating could be categorized into four classes [122]; C1/S1 (low salt concentrations suitable for irrigation/without the risk of exchangeable Na), C2/S2 (moderate salinity level and can be utilized without any special treatment/slight Na hazard in some finely–grained soils with high cation exchange potential), C3/S3 (high salinity level and not suitable for irrigation except when special management measures are implemented/high Na exchangeable potential) and C4/S4 (Extremely high salinity content and not advisable for utilization except when a distinct remediation approach is being implemented/extremely poor for irrigation and can only be considered for plants with high salt tolerance capacity) [122]. As shown in Fig. 13a, the groundwater samples either fell into class C1/S1 or C2/S1, which suggests low Na contents in the examined groundwater. This means that the groundwaters in the Ojo region are appropriate for irrigation operations without adversely affecting all types of soils and plants, and that no specific water treatment was required.

4.7.2. (ii) Soluble sodium percentage (SSP)

The SSP is an essential index for quantifying the risks associated with sodium in relation to the quality of water for irrigation activities [123]. Elevated SSP in groundwater used for irrigation purpose may impair plant growth and limit the permeability level of the soil [124]. The SSP values of ten groundwater resources were investigated in this study. SSP values less than 60 % and greater than 60 % are considered suitable and unsuitable, respectively, for irrigation purposes. The SSP values in the present study, as provided in Table S6, ranged from 32.205 %–52.883 % (meq/l), which confirmed the suitability of groundwater for irrigation purposes. For a clearer context, the Wilcox diagram (Fig. 13b) was employed to plot the SPP values against the EC values. All the plotted values fell within the category of "good to excellent," which demonstrates that long–term utilization of the groundwater resources is associated with negligible risk.

Table 5
Correlation coefficients of physicochemical, hydrogeochemical and heavy metal parameters in groundwater from Ojo district.

	Temp	pH	TDS	TH	EC	BOD	COD	Na	Mg	Ca	K	SO4	NO3	Cl	HCO3	As	Cd	Cr	Cu	Fe	Pb	Mn	Ni	Zn
Temp	1																							
pH	.094	1																						
TDS	−.531	.328	1																					
TH	−.485	.303	.991**	1																				
EC	.526	−.321	−.999**	−.989**	1																			
BOD	−.459	.361	.963**	.959**	−.960**	1																		
COD	−.096	.063	.759**	.799**	−.758**	.686*	1																	
Na	.149	.202	.629*	.709*	−.623*	.611*	.899**	1																
Mg	−.480	.241	.943**	.963**	−.936**	.883**	.824**	.739**	1															
Ca	−.513	.327	.993**	.986**	−.993**	.974**	.729**	.613*	.933**	1														
K	.558*	−.212	−.961**	−.948**	.958**	−.948**	−.736**	−.593*	−.917**	−.951**	1													
SO4	−.493	.333	.998**	.994**	−.998**	.966**	.779**	.662*	.950**	.994**	−.960**	1												
NO3	−.190	.263	.847**	.849**	−.860**	.809**	.744**	.634*	.751**	.865**	−.723**	.856**	1											
Cl	−.493	.333	.998**	.994**	−.998**	.966**	.779**	.662*	.950**	.994**	−.960**	.998**	.856**	1										
HCO3	−.596*	.385	.968**	.958**	−.968**	.954**	.631*	.524	.876**	.974**	−.913**	.964**	.815**	.964**	1									
As	.606*	−.060	−.915**	−.902**	.914**	−.901**	−.701*	−.522	−.870**	−.912**	.980**	−.914**	−.682*	−.914**	−.878**	1								
Cd	.658*	−.327	−.922**	−.889**	.924**	−.929**	−.497	−.341	−.781**	−.936**	.868**	−.909**	−.790**	−.909**	−.964**	.842**	1							
Cr	−.608*	.359	.676*	.647*	−.669*	.546	.526	.295	.674*	.639*	−.565*	.660*	.512	.660*	.677*	−.513	−.641*	1						
Cu	.312	.138	.479	.484	−.487	.584*	.597*	.563*	.386	.513	−.485	.508	.677*	.508	.396	−.459	−.401	.015	1					
Fe	−.126	.370	.776**	.775**	−.769**	.836**	.724**	.640*	.764**	.797**	−.785**	.799**	.698*	.799**	.713*	−.736**	−.674*	.489	.771**	1				
Pb	.520	.016	−.823**	−.851**	.822**	−.810**	−.755**	−.622*	−.792**	−.824**	.827**	−.828**	−.704*	−.828**	−.843**	.864**	.764**	−.558*	−.416	−.641*	1			
Mn	.552*	−.284	−.973**	−.967**	.966**	−.963**	−.757**	−.620*	−.947**	−.967**	.960**	−.973**	−.769**	−.973**	−.934**	.916**	.899**	−.696*	−.489	−.842**	.825**	1		
Ni	.485	−.382	−.126	−.049	.111	−.116	.186	.353	−.098	−.114	.190	−.108	.222	−.108	−.191	.192	.220	−.490	.279	−.221	.030	.209	1	
Zn	.542	−.152	−.918**	−.927**	.916**	−.914**	−.761**	−.631*	−.867**	−.914**	.940**	−.922**	−.730**	−.922**	−.920**	.949**	.846**	−.581*	−.468	−.742**	.961**	.775*	.144	1

*. Significance level of 0.05 (1–tailed)
**. Significance level of 0.01 (1–tailed)
The shaded numbers indicate positive correlations

4.7.3. (iii) permeability index (P.I)

The P.I is a measure of the ability of soil to transmit water, which reflects how easily water can flow through the soil. Soils with high permeability have good drainage, while soils with low permeability retain water more readily [6]. While low permeability soils tend to retain water more easily, high permeability soils drain well. The extended use of irrigation water can affect soil permeability; important variables include soil type, TDS, and the $NaHCO_3^-$ ratio [125]. The P.I scores can be apportioned into three classes, as shown in the Doneen chart (Fig. 13c). The P.I values of this study range from 55.484 %–70.723 % meq/l (Table S6), which falls into the class II (good category). This implies that the groundwater samples for irrigation purposes have about 25 %–75 % permeability potential.

4.7.4. (iv) Magnesium hazard ratio (MHR) and Kelly ratio (K.R)

The concentration of Mg^{2+} is one of the major indicators for determining the suitability of water for irrigation purposes. Generally, Ca^{2+} and Mg^{2+} maintain equilibrium in aquifer system due to lithogenic processes that involve rock–water interactions [9]. However, significantly high Mg^{2+} level than Ca^{2+} in irrigation water could limit crop yield due to the high salinity in the soil which is not favourable for plant development [126]. The MHR values that determine the suitability of groundwater for irrigation are broadly categorized into classes (Table 1). In this study, the MHR values ranged from 27.682 %–32.069 % meq/l, (MHR <50), which suggests that the examined groundwater samples are good for irrigation purposes. Similarly, the Kelly ratio (K.R) which involves measuring Na^+ against Ca^{2+} and Mg^{2+} was utilized to further determine the suitability of groundwater for irrigation purposes. A K.R score less than or greater than 1 suggests good and bad water respectively. The K.R values of this study were < 1 except for those of WE2 (1.114) and WE5 (1.122). This implies that 80 % of the groundwater resources are good, while 20 % are poor and unfit for irrigation practices (due to alkali abundance) except when treated.

4.8. Source apportionment of groundwater parameters

4.8.1. Pearson correlation matrix (PCM)

The Pearson correlation matrix was employed to examine the linear relationship between the groundwater parameters and their probable distribution sources [36,127]. Strong positive correlations indicate that two water parameters have the same origin, are mutually dependent on one another, and share identical chemical characteristics during transportation [35]. Conversely, a negative correlation implies that the water parameters lack the aforementioned characteristics. Correlation coefficients of the parameters of the groundwater from the Ojo district are presented in Table 5. Strong positive correlations were obtained between Temp vs. As (0.606) and Cd (0.658) at $P < 0.05$. TDS correlated positively with TH (0.991), BOD (0.963), COD (0.759), Mg^{2+} (0.943), Ca^{2+} (0.993), SO_4^{2-} (0.998), NO_3^- (0.847), Cl^- (0.998), HCO_3^- (0.968), Fe (0.776) at $P < 0.01$, Na^+ (0.629), and Cr (0.676) at $P < 0.05$. TH showed strong positive correlation with BOD (0.959), COD (0.799), Mg^{2+} (0.963), Ca^{2+} (0.986), SO_4^- (0.994), NO_3^- (0.849), Cl^- (0.994), HCO_3^- (0.958), Fe (0.775) at $P < 0.01$, Na^+ (0.709), and Cr (0.647) at $P < 0.05$. EC correlated strongly with K^+ (0.958), As (0.914), Cd (0.924), Pb (0.822), Mn (0.966), and Zn (0.916) at $P < 0.01$. BOD correlated with COD (0.686), Na^+ (0.611) at $P < 0.05$, Mg^{2+} (0.883), Ca^{2+} (0.974), SO_4^- (0.966), NO_3^- (0.809), Cl^- (0.966), HCO_3^- (0.954), and Fe (0.836) at $P < 0.01$. COD showed correlation trends with water variables comparable to those of BOD. Na^+ correlated with Mg^{2+} (0.739, $P < 0.01$), Ca^{2+} (0.613), SO_4^- (0.662), NO_3^- (0.634), Cl^- (0.662), and Fe (0.640) at $P < 0.05$. Mg^{2+} showed strong correlations with Ca^{2+}, SO_4^-, NO_3^-, Cl^-, HCO_3^-, Fe at $P < 0.01$ and Cr (0.639, $P < 0.05$). K was positively correlated with five (5) heavy metals (As = 0.980, Cd = 0.868, Pb = 0.827, Mn = 0.960, and Zn = 0.940) at $P < 0.01$. SO4 showed strong positive correlations with NO_3^- (0.856), Cl^- (0.998), and HCO_3^- (0.964) at $P < 0.01$. Positive correlations were obtained between NO_3^-, Cl^-, and HCO_3^-. As was positively correlated with Cd (0.842), Pb (0.864), Mn (0.916), and Zn (0.949), while Cd was strongly correlated with Pb (0.764), Mn (0.899), and Zn (0.849) at $P < 0.01$. Cu correlated positively with Fe (0.771), while Pb correlated strongly with Mn (0.825) and Zn (0.961) at $P < 0.01$. Finally, Mn and Zn (0.775, $P < 0.05$) were positively correlated. Temperature (except for As and Cd) and pH showed no correlation with the water parameters, implying that temperature has an insignificant influence on groundwater geochemistry while pH is influenced by numerous external factors and not groundwater parameters. The strong correlations of TDS with other parameters signify mineralization and anthropogenic phenomena, although the negative correlation with K (−0.961) confirmed the geogenic origin of K [128]. The strong correlations between silicate ions (Cl^-—SO_4^{2-}—HCO_3^-—NO_3^-) imply interdependence and similar sources of origin. Moreover, a strong correlation between NO_3^- and HCO_3^- confirmed the precipitation infiltration in the aquifer system [128]. Furthermore, the correlations between TH and silicate ions, Na^+, Mg^{2+}, and Ca^{2+} imply rock–water interactions, mineral precipitation, silicate, and dolomite weathering [34]. The linear relationships of TH with Ca^{2+} and Mg^{2+} implies that these cations are responsible for groundwater hardness in the study area. The strong correlation between Na^+ and Cl^- may be the consequence of seawater intrusion from nearby water bodies, especially the ocean and lagoons, given the coastal nature of the investigated area. High concentrations of Na+ and Cl− may also be related to mineralization, specifically the breakdown of halite [34]. The correlations between As and other heavy metals such as Cd, Pb, and Mn imply similar sources of origin and are likely due to numerous anthropogenic activities within the study area. Fe showed no significant correlation with water parameters, which suggests that Fe could be of geogenic origin. The strong correlation between Zn and Pb in borehole water denotes similar sources, mostly from deteriorated galvanized metals. When acidic water comes into contact with galvanized metals such as zinc, iron, and small concentrations of Pb, the exposed surface area slowly dissolves. If drinking water is kept in metal containers or passes through lead pipes that have been zinc–coated to prevent rust, the quantities of Zn and Pb may increase. This assertion gave credence to the outcome of this study because the plumbing set up for a borehole requires leaded pipes coated in zinc. The low positive and high negative correlations of some heavy metals such as Cr, Cu, and Ni suggest multiple sources of origin and no interelement dependence or similar chemical behavior. This finding supports the hypothesis of Kükrer et al. [129] that heavy metals are influenced by several complex variables and could be confirmed when two elements showed a negative or weak positive

correlation. Moreover, their sources could be a result of natural processes, including weathering and atmospheric deposition, or anthropogenic activities, including agricultural practices and industrial activities that are being carried out in Ojo district. The multivariate assessment was conducted in the next subsection to offer more detailed and precise information regarding the source allocation of water parameters in groundwater.

4.8.2. Factor analysis of groundwater parameters through the principal components (PCs) criterion

The factor analysis (FA) was performed to precisely understand the potential origin and geochemical distribution patterns of the groundwater parameters. Additionally, FA was employed to minimize the extensivity of large data sets for concision while preserving the originality of the data [35,36,47]. The PCs of twenty–one groundwater variables, eigenvalues, variances, KMO, and BTS are depicted in Table 6. A KMO equal to or greater than 0.6 implies that the data sets are adequately enough for FA, while a BTS value of $P < 0.05$ is considered acceptable [39]. The obtained values (KMO = 0.705 and BTS = 0.000) confirmed the appropriateness and sufficiency of the data sets for the present investigation. The substantiality of each component was obtained via the eigenvalues, such that an eigenvalue of less than one was considered irrelevant [130]. The eigenvalues range from 1.986 to 16.205. The screen plot displayed in Fig. 14a shows that three (3) variables had eigenvalues greater than 1, while the others were tailed off. This justifies the three (3) principal components retained in this study. The graphical representation of the component plots in rotated space provided in Fig. 14b shows the correlations between the heavy metal variables. The 89.67 % cumulative variance obtained demonstrates high variabilities and transitions of groundwater parameters. Moreover, a factor loading above 0.500 is considered significant, while a factor loading below 0.500 is classified as insignificant. Furthermore, factor loadings higher than 0.750 are categorized as high, indicating substantial involvement of a variable in the examined group. The factor loadings between 0.500 and 0.700 are considered medium, while those below 0.500 are regarded as weak [23]. In this study, PC1 accounted for 67.519 % of the total variance and was strongly loaded with factors of TDS (0.957), TH (0.950), BOD (0.912), COD (0.709), Na^+ (0.527), Mg^{2+} (0.916), Ca^{2+}, SO_4^- (0.949), NO_3^- (0.749), Cl^- (0.949), HCO_3^- (0.945), Cr (0.689), Fe (0.686), Pb (0.899), and Zn (950). This result is similar to those obtained in Table 5 (correlation matrix). PC2 is responsible for 13.897 % of the cumulative variances and is loaded with high factors of Temp (0.693), COD (0.558), Na^+ (0.719), Cu (0.788), and Ni (0.656). PC3, which explains only 8.277 % of the aggregated variance, was loaded with high factor of only pH (0.962), similar to the outcome obtained in the correlation matrix (Table 5), where pH showed no strong positive correlation with any of the parameters.

The high loads of these factors (TDS, TH, BOD, COD, Na^+, Mg^{2+}, Ca^{2+}, SO_4^-, Cl^-, HCO_3^-), except for NO_3^- and some heavy metals (Cr, Fe, Pb, and Zn), in PC1 denote the prevalence or occurrence of mineralization (geogenic phenomena), seawater intrusion, and rock

Table 6
Principal component analysis of groundwater parameters.

	Rotated Component Matrix[a]		
	PC1	PC2	PC3
Temp	−0.703	**.693**	0.115
pH	0.118	0.102	**.930**
TDS	**.957**	0.182	0.192
TH	**.950**	0.246	0.143
EC	−0.955	−0.189	−0.183
BOD	**.912**	0.244	0.235
COD	**.709**	**.558**	−0.056
Na^+	**.527**	**.719**	0.008
Mg^{2+}	**.916**	0.211	0.115
Ca^{2+}	**.949**	0.201	0.199
K^+	−0.953	−0.140	−0.104
SO_4^{2-}	**.949**	0.225	0.196
NO_3^-	**.746**	0.484	0.127
Cl^-	**.949**	0.225	0.196
HCO_3^-	**.945**	0.067	0.233
As	−0.953	−0.080	0.030
Cd	−0.911	0.026	−0.226
Cr	**.689**	−0.244	0.359
Cu	0.343	**.788**	0.140
Fe	**.686**	0.439	0.397
Pb	**.899**	−0.154	0.162
Mn	−0.953	−0.150	−0.199
Ni	−0.183	**.656**	−0.569
Zn	**.950**	−0.151	−0.011
Eigen values	16.205	3.331	1.986
Variance (%)	67.519	13.878	8.277
Total variance (%)	67.519	81.397	89.673
KMO (indicator of sampling adequacy)			**.705**
Bartlett's Test of Sphericity (Sig)			**.000**

Extraction (Principal component analysis), Rotation type (Varimax with Kaiser Normalization).
[a] Rotation converged in 7 iterations.

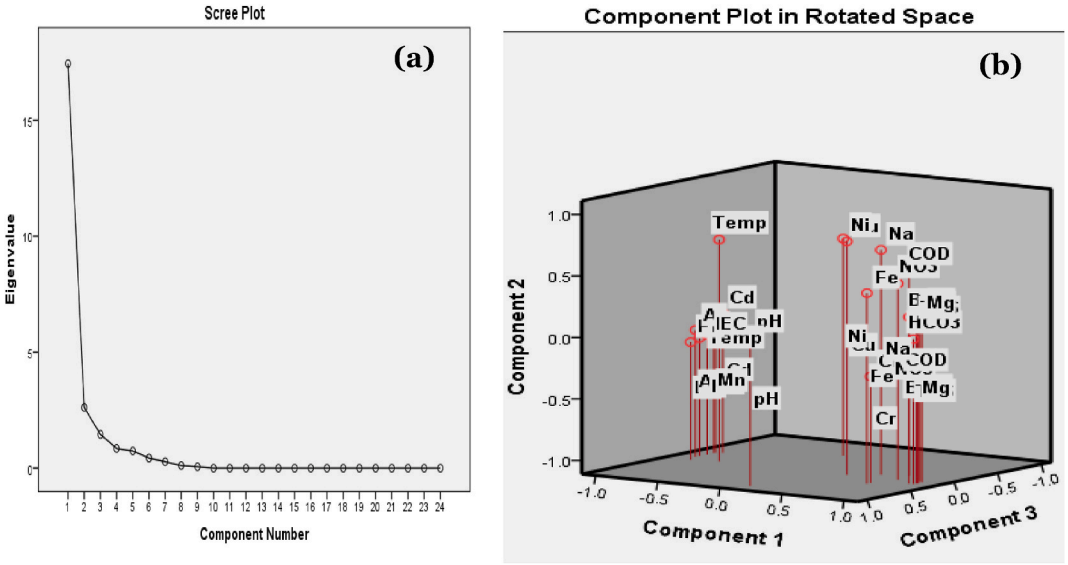

Fig. 14. (a)Screen plots showing the eigen values (b) Component plots in rotated spaces.

weathering. The lithological constituents of the study area and the heavy metal factors in PC1 demonstrate that mineral or rock weathering events are not responsible for the heavy metals in the groundwater of this study. The source of NO_3^- in groundwater can be traced to anthropogenic activities such as the seepage of fertilizer from agricultural lands, decaying plant debris, refuse dumps, sewage systems, and animal feedlots [87]. Mohammed et al. [32] reported that Ca fertilizers tend to release NO_3^- into groundwater, whereas Ca and CN− are combined to produce NH_3 and $CaCO_3$, subsequently NH3 is oxidized to NO_3^-. High loads of Cr, Pb, and Fe in groundwater demonstrate different anthropogenic sources, including toxic leachate from households, landfill and chrome plating liquid wastes, and industrial effluents that eventually seeped into groundwater [35]. Jolaosho et al. [36] asserted that construction and automobile materials, as well as plumbing pipes erected in water systems, could also result in elevated loads of Pb, Cr, and Zn in groundwater. The extensive engagement of farmers in agricultural activities on vast areas of lands within Ojo settlement—considering the intensive utilization of agrochemicals such as pesticides or fertilizers—might have led to high seepage of these elements into the groundwater

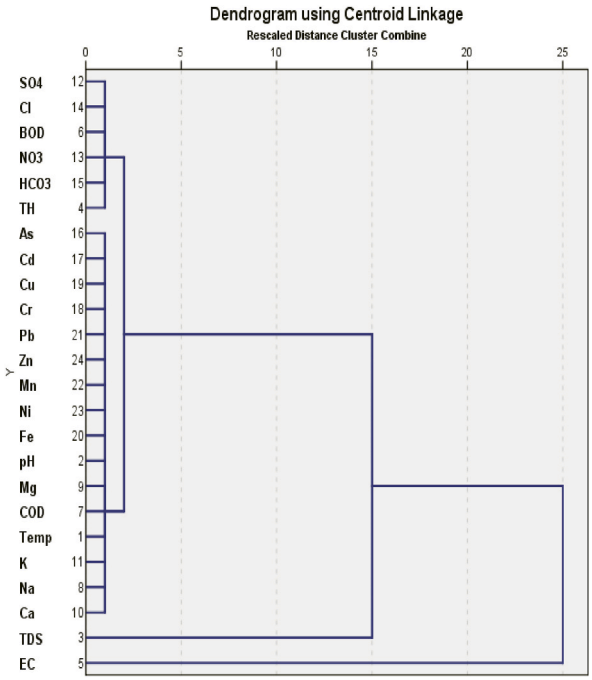

Fig. 15. Dendrograms showing the clusters of water variables in groundwater.

[131]. In addition, anthropogenic influences, including the lithium battery and painting materials, pipes and galvanized metals rusted in groundwater systems, sewage systems, and car exhaust, are all potential sources of Zn and Pb [36]. The factor loading of Na^+ in PC2 further confirmed the seawater deposits and mineral weathering of Na–bearing rocks. Similarly, the high loads of Cu and Ni could be attributed to the use of corrosive plumbing materials, and brass faucets. Cerchier et al. [132] reported that Cu is a water toxicant and is highly present in the antifouling materials used by shipping industries. Conversely, Ni could be a result of geogenic phenomena [133], such as weathering and atmospheric evaporation of mineral soils and rocks that are rich in Ni. Given that pH is the only factor in PC3, it is apparent that the pH is a result of external influences rather than geological processes.

4.8.3. Cluster analysis (CA) of groundwater parameters

Hierarchical cluster analysis via centroid linkage and the Euclidian distance technique was performed to determine the factorial groupings and categorize the groundwater parameters into clusters based on similarities in chemical properties [35,134]. These clusters allow for the determination of the relationship as well as the identification of the origin of the groundwater parameters, whether lithogenic or anthropogenic. The identified groundwater clusters are represented as dendrograms, as provided in Fig. 15. The water parameters in groundwater generated three (3) major clusters and two subclusters within a distance of 0–10. Cluster 1 comprised of 90.47 % (19 samples) of the water parameters, of which two subclusters (Subcluster 1 = SO4, Cl, BOD, NO3, HCO3, and TH; Subcluster 2 = As, Cd, Cu, Cr, Pb, Zn, Mn, Ni, Fe, pH, Mg, COD, Temp, K, Na, and Ca) were formed. This points to the fact that the hydrogeochemical parameters, particularly silicate ions and the heavy metals in the investigated aquifer groundwater originated from different media sources, both of which involves geogenic and anthropogenic processes. Clusters 2 and 3 are loaded with TDS and EC, respectively.

4.9. Health risk evaluation of heavy metals in groundwater

4.9.1. Daily ingestion rates and exposure pathways

The ADD is regarded as the daily exposure of human populations to certain concentrations of heavy metals in particles such as water through ingestion and dermal routes (USEPA, 1997). For children, the contributions of each metal to ADD ingestion and ADD dermal in boreholes and well water samples are provided in Table S7. Based on the results, Fe contributed mostly to ADD ingestion in BH1 (3.24×10^{-4}), BH2 (2.70×10^{-7}), BH3 (3.06×10^{-7}), BH4 (2.34×10^{-7}), WE1 (3.96×10^{-6}), WE2 (4.86×10^{-7}), WE3 (4.50×10^{-7}), WE3 (3.60×10^{-7}), WE4 (3.60×10^{-7}) and WE5 (3.24×10^{-7}) while Mn was highest in BH5 (2.88×10^{-7}). As had the highest contribution to ADD_{dermal} in BH1 (3.24×10^{-4}), BH2 (2.70×10^{-7}), BH3 (3.06×10^{-7}), BH4 (2.34×10^{-7}), WE1 (3.96×10^{-6}), WE2 (4.86×10^{-7}), WE3 (4.50×10^{-7}), WE3 (3.60×10^{-7}), WE4 (3.60×10^{-7}) and WE5 (3.24×10^{-7}) while Mn was highest in BH5 (2.88×10^{-7}). In reference to adult category, the ADDs (ingestion and dermal contact) are provided in Table S7. Fe contributed the most to $ADD_{ingestion}$ in BH1 (3.60×10^{-4}), BH3 (3.40×10^{-4}), and BH3 (2.60×10^{-4}). The $ADD_{ingestion}$ for As and Mn was highest in BH2 (3.10×10^{-4}) and BH5 (3.20×10^{-4}). Fe contributed mostly to $ADD_{ingestion}$ in WE1 (4.40×10^{-4}), WE2 (5.40×10^{-4}), WE3 (4.50×10^{-7}), WE3 (5.0×10^{-4}), WE4 (4.0×10^{-4}) and WE5 (3.60×10^{-4}). As had the highest contribution to ADD_{dermal} in BH1 to BH5 while Fe contributed the most to the ADD_{dermal} in WE1 to WE5 (Table S8). Most of the ADDs of heavy metals except for As, were lower than RfDs. Figs. S1a and S1b show the ADDs distributions (%) of heavy metals in groundwater for children and adult group. The results of the study showed that the dermal route contributed very little to the daily exposure of adults and children to heavy metals in groundwater, with ingestion pathways accounting for more than 99 % (borehole) and range of 75 %–82 % (well) of the total. This signifies that exposure to groundwater through the ingestion pathway has a greater chance of posing health risks to children and adults than does the dermal exposure route.

4.9.2. Noncancer risk of heavy metals (hazard quotient and hazard index)

Table S9 depicts the calculated noncancer risks of heavy metals in groundwater. The HQ and HI are important parameters that estimate the noncarcinogenic health implications of the heavy metals in water from a specific location [35,36]. Human are considered at risk when exposed to highly toxic contaminants. This could be said when the HQ and HI values are above 1. The HI of this study was computed by summing the calculated hazard quotient (HQ) values. In the children's category, the HQ values (ingestion dermal) were below 1 were for all the metals in the examined groundwater samples. Similarly, the HI values (ingestion + dermal) ranged from 0.001 to 0.003 for all the groundwater samples. This result implies that exposure to heavy metals in groundwater is unlikely to pose non-cancer risks to children. Conversely, the calculated $HQ_{ingestion}$ in the adult category showed that As exceeded the threshold of 1 ($HQ > 1$) in three groundwater samples (BH1, BH2, and BH5), which was not the case with the HQ_{dermal} values ($HQ_{dermal} < 1$). Jolaosho et al. [35] reported that exposure to As for a considerable period of time could result in several health complications, such as skin lesions, negative cognitive development, endocrine, renal, and cardiovascular system impairment, hematopoietic dysfunction, respiratory system damage, diabetes, and even death. Furthermore, the calculated HI values (ingestion + dermal) of the three groundwater samples [BH1 (1.131), BH2 (1.149), and BH5 (1.290)] exceeded the threshold of 1 ($HI \leq 1$). These results clearly showed that exposure to some borehole water samples could cause noncancer adverse effects in adults, which could be attributed to the high concentrations of As. Tong et al. [135] reported a HQ As value of 1.53 for adult age group, which contributed significantly to the noncancer risks associated with drinking groundwater in China. The noncancer health risk outcome of this study also corresponds to those of Liu and Ma [136], where groundwater within a catchment river in North China showed noncancer risk potential. Similarly, Zhu et al. [137] reported in their finding that, based on USEPA standard values, approximately 15 % of the total groundwater samples in the Yinchuan region of China are capable of causing noncarcinogenic defects.

4.9.3. Carcinogenic health risk of heavy metals (ingestion and dermal contact)

Table S10 shows the carcinogenic risk of heavy metals in groundwater. Based on the classification of international agency research for cancer [138], the five (5) heavy metals that are capable of causing cancer (number 1 carcinogens) were considered in this study. Generally, the values of 1.00×10^{-6} [cancer risk (CR)] and 1.00×10^{-4} [lifetime cancer risk (LCR)] have been considered the minimum and maximum allowable limits [35,39,62]. This infers that the cancer risk of 1 person out of 1,000,000 to 1 person out of 10,000 is acceptable [39,62,65]. However, values above the allowable limits indicate a high likelihood of cancer risk in humans [36]. In the children category, CR values (ingestion and dermal) of each carcinogen in the groundwater samples were lower than the threshold limit of 1.00×10^{-6} for a single carcinogen. The children LCR (ingestion + dermal) values range from 2.39×10^{-7} to 9.53×10^{-7}. These values were lower than the 1.00×10^{-4} threshold limit established for multiple carcinogens. This indicates that exposure of children to groundwater from Ojo district would not result in cancer risks. In contrast, the adult's $CR_{ingestion}$ values obtained for As, Cd, Cr, and Ni exceeded the threshold limit (1.00×10^{-6}) for a single carcinogen in all the groundwater samples (BH1 to WE5). This could not be said for the dermal exposure route, where the CR values were within their respective minimum limits. In addition, the LCR (ingestion + dermal) values of all the examined groundwater exceeded the threshold limit (1.00×10^{-4}) for multiple carcinogens in water. It could, thus, be inferred that in the adult category, there is a possibility of cancer risks due to elevated concentrations of some carcinogens (As, Cd, Cr, and Ni) in all the groundwater samples. Carcinogenic health risks for adults were also reported in groundwater from several regions in China [135–137]. As has been linked to skin, bladder, and lung cancer [35,39], while Cd has been linked to several cancers, including lung, renal, pancreatic, and prostate cancer [138]. Cr is capable of causing paranasal sinuses, lung, and nasal cavities, while the likelihood of nasal and lung cancers is associated with Ni exposure [139].

5. Conclusion

This study examines ten groundwater from the Ojo district for twenty–four (24) physicochemical, hydrogeochemical, and heavy metal parameters to determine the processes and mechanisms influencing geochemical evolution, water types and facies, consumption and irrigation suitability, contamination degree, source allocation, and potential health risks. The findings underscore the critical need for ongoing monitoring and intervention strategies to safeguard this vital resource, given its implications for public health and environmental sustainability. The groundwater parameters of the samples generally adhered to international standard limits, suggesting that the groundwater is predominantly of acceptable quality. The ion concentration patterns revealed a dominance of sodium (Na^{+}), calcium (Ca^{2+}), and bicarbonate ($HCO3-$), which signifies the influence of geological weathering processes and mineralogical interactions within the aquifer systems. The results from the Piper diagram classified the groundwater into distinct geochemical facies, predominantly characterized by Ca–Mg–$HCO3-$ types, highlighting the complex interplay of natural processes that govern groundwater chemistry. In addition, the study identified significant concerns regarding heavy metal contamination. The heavy metal concentrations hierarchy were; Fe > Mn > Ni > Zn > Pb > As > Cd > Cr > Cu, with the concentrations of Pb, Mn, and Ni exceeding their respective permissible limits. This raises concern about potential risks, emphasizing the need for urgent attention to the sources of these contaminants. The pollution index assessments revealed that while a majority of the groundwater samples were categorized as good quality, substantial samples (30 %) were moderately contaminated. The GWQI and WPI illustrated a concerning trend—only 10 % of the samples were classified as highly clean, with approximately 80 % falling into the poor to extremely unclean categories, indicating that the groundwater is not suitable for consumption without proper treatment. This finding is especially alarming given the potential health implications associated with the consumption of contaminated water. The health risk assessment further elucidates the exposure patterns of heavy metals, underscoring ingestion as the primary route of exposure. The HQ and HI of children indicated a low likelihood of adverse non–cancer health effects. Conversely, the adult population exhibited concerning HQ and HI values, particularly associated with arsenic (As), cadmium (Cd), chromium (Cr), and nickel (Ni), which could pose significant cancer risks. While the groundwater in the Ojo district reflects certain qualities that align with international standards, the persistent contamination by heavy metals poses a serious threat to public health. Our findings indicate an urgent need for improved water management practices, stringent monitoring, and pollution control measures aimed at reducing heavy metal concentrations in groundwater. Furthermore, public health strategies should prioritize the education of local communities about the potential health risks associated with contaminated water and the importance of water treatment prior to consumption. Given the multifaceted sources of groundwater contamination, it is imperative to implement a holistic approach for water management and conservation to ensure the long-term integrity of this essential resource. This would involve collaboration among environmental scientists, health officials, and local stakeholders to devise effective remediation strategies and sustainable water management practices. The study advocates for continuous monitoring and assessment of groundwater quality to safeguard human health and preserve this essential resource for future generations. The findings emphasize the imperative of proactive measures to ensure that the groundwater in the Ojo district can be safely utilized, ultimately contributing to the health and wellbeing of the local community.

5.1. Implications for the study

5.1.1. Ecological and community health concerns

This study revealed that groundwater resources from the Ojo district are capable of causing acute toxicity (ecological and human health) due to the high heavy metal concentrations. The hydrogeochemical indices revealed the silicate weathering and seawater intrusion are the part of factors regulating the aquifer systems in Ojo District. The chemometric–based assessment dedicated to identifying the potential sources and the associated adverse effects of the groundwater parameters in the investigated aquifer system confirmed the roles played by both lithogenic phenomena such as rock–water interactions, mineralization and weathering as well as

several anthropogenic processes particularly industrial and agricultural activities. In addition, the leaching of inorganic chemicals into the groundwater due to agrochemicals used for farming activities and household wastes within the study region poses health concerns for the community as a whole.

5.1.2. Theoretical implications

This novel investigation contributes to the theoretical knowledge and comprehension of the chemical parameters of groundwater. Moreover, the present findings shed light on the mechanisms and factors governing the hydrochemistry of groundwater, including ionic exchange processes, rock–water interactions, seawater dynamics, weathering events, and mineralization. The sources of contaminants that were discovered provide clear reflections on the intricate interactions between geogenic and anthropogenic processes that influence the quality of the groundwater.

5.1.3. Practical implications

This outcome of this investigation justifies the need for the urgent implementation of effective conservation measures for sustainability and natural resource protection. Given that the results of the study revealed carcinogenic and noncarcinogenic health implications, there is a need for urgent water treatment, remediation, and continuous monitoring of groundwater resources in the study region and its environment. The identified origins of contaminants can help to directly focus on mitigation initiatives and help to shape policy choices that will minimize negative effects on the environment and safeguard public health.

5.2. Uncertainties and drawbacks

Due to the personalities of the residents, nature, organizational structure, and management system of the study area, the proximity to freely access the entire available groundwater system was not feasible, as there were restrictions to some ends, mainly in the military zone of Ojo district. Notably, a particular number of samples and, preferably, a follow–up examination should be used to indicate the contamination degree of heavy metals and metalloids in the human body as well as the environment. There are about 23 public groundwater erections in the Ojo District; however, a limited number of 10 were assessed for the purpose of this study due to the aforementioned constraints. The inability to comprehensively evaluate all the ground waters might have reduced the quality of the results, which could be considered a gap in the study. In addition, the study was not able to interview the residents (qualitative approach) or seek the opinions or perceptions of the respondents through survey questionnaires about groundwater usage—questions associated with mode of water treatment, average daily dose, and water utilization—in all contexts deemed essential for the purpose of this study. Lastly, the predisposing factors or differences in the physiological abilities (tolerance level) of individuals to withstand adversity might play roles in exposure to noncarcinogenic and carcinogenic risks. As a result, it is possible that the severities in reference to the health risk evaluations in this study were marginally overstated.

5.3. Recommendation for future studies

This assessment provides novel ideas yet fascinating directions for future investigations. However, studies on microbial counts in groundwater and heavy metal contents and health risk analysis of sediment within the study area are essential due to the high level of agricultural practices within the study area and the overall geological composition. Future studies could integrate advanced spatial and surveillance approaches, particularly remote sensing and machine learning, to further comprehend the dynamic factors influencing groundwater resources in the study area. The safeguarding of water resources and the health of the general population could be improved by the implementation of more sophisticated strategies that make use of these sophisticated instruments, thus providing a basis for long–term water management techniques. These cutting–edge techniques have an enormous capacity to guarantee long–term resilience to problems associated with groundwater quality and pollution.

Data availability statement

Data will be made available on request.

Funding

This research was not funded by any organization or individual.

CRediT authorship contribution statement

Toheeb Lekan Jolaosho: Writing – review & editing, Writing – original draft, Visualization, Validation, Supervision, Software, Resources, Project administration, Methodology, Investigation, Funding acquisition, Formal analysis, Data curation, Conceptualization. **Adejuwon Ayomide Mustapha:** Writing – review & editing, Software, Methodology, Formal analysis, Data curation. **Samuel Todeyon Hundeyin:** Writing – review & editing, Visualization, Methodology, Funding acquisition, Formal analysis, Data curation.

Declaration of competing interest

The authors declare that they have no known competing financial interests or personal relationships that could have appeared to influence the work reported in this paper.

Appendix A. Supplementary data

Supplementary data to this article can be found online at https://doi.org/10.1016/j.heliyon.2024.e38364.

References

[1] A. Mukherjee, B.R. Scanlon, A. Aureli, S. Langan, H. Guo, A. McKenzie, Global groundwater: from scarcity to security through sustainability and solutions, in: Global Groundwater, Elsevier, 2021, pp. 3–20.
[2] X. Jia, D. O'Connor, D. Hou, Y. Jin, G. Li, C. Zheng, J. Luo, Groundwater depletion and contamination: spatial distribution of groundwater resources sustainability in China, Sci. Total Environ. 672 (2019) 551–562.
[3] O.B. Akpor, M. Muchie, Remediation of heavy metals in drinking water and wastewater treatment systems: processes and applications, Int. J. Phys. Sci. 5 (12) (2010) 1807–1817.
[4] D. Machiwal, M.K. Jha, V.P. Singh, C. Mohan, Assessment and mapping of groundwater vulnerability to pollution: current status and challenges, Earth Sci. Rev. 185 (2018) 901–927.
[5] N.M. Burri, R. Weatherl, C. Moeck, M. Schirmer, A review of threats to groundwater quality in the anthropocene, Sci. Total Environ. 684 (2019) 136–154.
[6] J. Singh, P. Yadav, A.K. Pal, V. Mishra, Water pollutants: origin and status, Sensors in water pollutants monitoring: Role of material (2020) 5–20.
[7] S. Issaka, M.A. Ashraf, Impact of soil erosion and degradation on water quality: a review, Geology, Ecology, and Landscapes 1 (1) (2017) 1–11.
[8] S. Swain, A.K. Taloor, L. Dhal, S. Sahoo, N. Al–Ansari, Impact of climate change on groundwater hydrology: a comprehensive review and current status of the Indian hydrogeology, Appl. Water Sci. 12 (6) (2022) 120.
[9] J. Iqbal, C. Su, A. Rashid, N. Yang, M.Y.J. Baloch, S.A. Talpur, M.M. Sajjad, Hydrogeochemical assessment of groundwater and suitability analysis for domestic and agricultural utility in Southern Punjab, Pakistan, Water 13 (24) (2021) 3589.
[10] J. Zhu, M. Li, M. Whelan, Phosphorus activators contribute to legacy phosphorus availability in agricultural soils: a review, Sci. Total Environ. 612 (2018) 522–537.
[11] H.A. Khalil, M.S. Hossain, E. Rosamah, N.A. Azli, N. Saddon, Y. Davoudpoura, R. Dungani, The role of soil properties and it's interaction towards quality plant fiber: a review, Renew. Sustain. Energy Rev. 43 (2015) 1006–1015.
[12] R.S. Kookana, P. Drechsel, P. Jamwal, J. Vanderzalm, Urbanisation and emerging economies: issues and potential solutions for water and food security, Sci. Total Environ. 732 (2020) 139057.
[13] S. Dos Santos, E.A. Adams, G. Neville, Y. Wada, A. De Sherbinin, E.M. Bernhardt, S.B. Adamo, Urban growth and water access in sub–Saharan Africa: progress, challenges, and emerging research directions, Sci. Total Environ. 607 (2017) 497–508.
[14] A.R. Gollakota, S. Gautam, C.M. Shu, Inconsistencies of e–waste management in developing nations–Facts and plausible solutions, J. Environ. Manag. 261 (2020) 110234.
[15] J. Ntajal, B. Höllermann, T. Falkenberg, T. Kistemann, M. Evers, Water and health nexus—land use dynamics, flooding, and water–borne diseases in the Odaw River basin, Ghana, Water 14 (3) (2022) 461.
[16] E.Y.Y. Chan, K.H.Y. Tong, C. Dubois, K. Mc Donnell, J.H. Kim, K.K.C. Hung, K.O. Kwok, Narrative review of primary preventive interventions against water–borne diseases: scientific evidence of health–EDRM in contexts with inadequate safe drinking water, Int. J. Environ. Res. Publ. Health 18 (23) (2021) 12268.
[17] B. Adelodun, F.O. Ajibade, J.O. Ighalo, G. Odey, R.G. Ibrahim, K.Y. Kareem, K.S. Choi, Assessment of socioeconomic inequality based on virus–contaminated water usage in developing countries: a review, Environ. Res. 192 (2021) 110309.
[18] M. Edwards, Fetal death and reduced birth rates associated with exposure to lead–contaminated drinking water, Environ. Sci. Technol. 48 (1) (2014) 739–746.
[19] I.R. Abubakar, Strategies for coping with inadequate domestic water supply in Abuja, Nigeria, Water Int. 43 (5) (2018) 570–590.
[20] O.B. Ezeudu, Urban sanitation in Nigeria: the past, current and future status of access, policies and institutions, Rev. Environ. Health 35 (2) (2020) 123–137.
[21] R. Haggerty, J. Sun, H. Yu, Y. Li, Application of machine learning in groundwater quality modeling–A comprehensive review, Water Res. (2023) 119745.
[22] S.M. Hosseini, E. Parizi, B. Ataie–Ashtiani, C.T. Simmons, Assessment of sustainable groundwater resources management using integrated environmental index: case studies across Iran, Sci. Total Environ. 676 (2019) 792–810.
[23] C.N. Mgbenu, J.C. Egbueri, The hydrogeochemical signatures, quality indices and health risk assessment of water resources in Umunya district, southeast Nigeria, Appl. Water Sci. 9 (1) (2019) 22.
[24] G. Gnanachandrasamy, C. Dushiyanthan, T. Jeyavel Rajakumar, Y. Zhou, Assessment of hydrogeochemical characteristics of groundwater in the lower vellar river basin: using geographical information system (GIS) and water quality index (WQI), Environ. Dev. Sustain. 22 (2020) 759–789.
[25] J. Ghani, Z. Ullah, J. Nawab, J. Iqbal, M. Waqas, A. Ali, M. Shah, Hydrogeochemical characterization, and suitability assessment of drinking groundwater: application of geostatistical approach and geographic information system, Front. Environ. Sci. 10 (2022) 874464.
[26] S.I. Abba, M.A. Yassin, S.M.H. Shah, J.C. Egbueri, H.E. Elzain, J.C. Agbasi, I.H. Aljundi, Trace element pollution tracking in the complex multi–aquifer groundwater system of Al–Hassa oasis (Saudi Arabia) using spatial, chemometric and index–based techniques, Environ. Res. (2024) 118320.
[27] P. Biswas, M. Hossain, P.K. Patra, Arsenic hydrogeochemistry, quality assessment, and associated health risks of groundwater through the novel water pollution index (WPI) and GIS approach, Groundwater for Sustainable Development 21 (2023) 100944.
[28] B. Ravindra, N. Subba Rao, E.N. Dhanamjaya Rao, Groundwater quality monitoring for assessment of pollution levels and potability using WPI and WQI methods from a part of Guntur district, Andhra Pradesh, India, Environ. Dev. Sustain. 25 (12) (2023) 14785–14815.
[29] B. Wang, Y. Wang, S. Wang, Improved water pollution index for determining spatiotemporal water quality dynamics: case study in the Erdao Songhua River Basin, China, Ecol. Indicat. 129 (2021) 107931.
[30] N.S. Rao, A. Dinakar, M. Sravanthi, B.K. Kumari, Geochemical characteristics and quality of groundwater evaluation for drinking, irrigation, and industrial purposes from a part of hard rock aquifer of South India, Environ. Sci. Pollut. Control Ser. 28 (2021) 31941–31961.
[31] J.C. Egbueri, C.N. Mgbenu, C.N. Chukwu, Investigating the hydrogeochemical processes and quality of water resources in Ojoto and environs using integrated classical methods, Modeling Earth Systems and Environment 5 (2019) 1443–1461.
[32] M.A. Mohammed, A. Eltijani, N.P. Szabó, P. Szűcs, Hydro–chemometrics of the Nubian Aquifer in Sudan: an integration of groundwater quality index, multivariate statistics, and human health risk assessment, Discover Water 3 (1) (2023) 15.
[33] R. Barzegar, A. Asghari Moghaddam, S. Soltani, E. Fijani, E. Tziritis, N. Kazemian, Heavy metal (loid) s in the groundwater of Shabestar area (NW Iran): source identification and health risk assessment, Exposure and Health 11 (2019) 251–265.
[34] S. Naidu, G. Gupta, R. Singh, K. Tahama, V.C. Erram, Hydrogeochemical processes regulating the groundwater quality and its suitability for drinking and irrigation purpose in parts of coastal Sindhudurg District, Maharashtra, J. Geol. Soc. India 97 (2021) 173–185.

[35] T.L. Jolaosho, I.O. Elegbede, P.E. Ndimele, T.E. Falebita, O.Y. Abolaji, I.O. Oladipupo, O.O. Isaac, Occurrence, distribution, source apportionment, ecological and health risk assessment of heavy metals in water, sediment, fish and prawn from Ojo River in Lagos, Nigeria, Environ. Monit. Assess. 196 (2) (2024) 109.
[36] T.L. Jolaosho, I.O. Elegbede, P.E. Ndimele, G.O. Mekuleyi, I.O. Oladipupo, A.A. Mustapha, Comprehensive geochemical assessment, probable ecological and human health risks of heavy metals in water and sediments from dredged and non–dredged Rivers in Lagos, Nigeria, Journal of Hazardous Materials Advances (2023) 100379.
[37] O.O. Okwa, Y.A. Oladipupo, A.R. Adesina, T.R. Ibukun, Estimation of geohelminthes prevalence in soil samples and risk factors to exposure in Ojo area of Lagos state, Nigeria, International Journal of Research and Scientific Innovation 10 (1) (2023) 58–67.
[38] M.A. Yusuf, T.A. Abiye, K.O. Ibrahim, H.O. Abubakar, Hydrogeochemical and salinity appraisal of surficial lens of freshwater aquifer along Lagos coastal belt, South West, Nigeria, Helliyon 7 (10) (2021).
[39] T.L. Jolaosho, I.O. Elegbede, S.L. Akintola, A.A. Jimoh, P.E. Ndimele, A.A. Mustapha, J.D. Adukonu, Bioaccumulation dynamics, noncarcinogenic and carcinogenic risks of heavy metals in commercially valuable shellfish and finfish species from the world largest floating slum, Makoko, Nigeria, Mar. Pollut. Bull. 207 (2024) 116807.
[40] K.D. Oyeyemi, A.P. Aizebeokhai, M.A. Oladunjoye, Integrated geophysical and geochemical investigations of saline water intrusion in a coastal alluvial terrain, southwestern Nigeria, Int. J. Appl. Environ. Sci. 10 (4) (2015) 1275–1288.
[41] A.A. Alabi, R. Bello, A.S. Ogungbe, H.O. Oyerinde, Determination of groundwater potential in Lagos State University, Ojo; using geoelectric methods (vertical electrical sounding and horizontal profiling), Report and opinion 2 (5) (2010) 68–75.
[42] G.P. Kruseman, Recharge from intermittent flow, in: Recharge of Phreatic Aquifers in (Semi–) Arid Areas, Routledge, 2017, pp. 145–184.
[43] A.K.A. Ahmed, M. El–Rawy, The impact of aquifer recharge on groundwater quality, in: Managed Aquifer Recharge in MENA Countries: Developments, Applications, Challenges, Strategies, and Sustainability, Springer International Publishing, Cham, 2024, pp. 207–222.
[44] M.O. Oloruntola, Geophysical and Hydrochemical Investigations of Abeokuta and Ikorodu Areas of Southwestern Nigeria, 2012 (Doctoral Dissertation).
[45] N. Zabbey, F.D. Giadom, B.B. Babatunde, Nigerian coastal environments, in: World Seas: an Environmental Evaluation, Academic Press, 2019, pp. 835–854.
[46] A. Akingboye, Geohydraulic characteristics and groundwater vulnerability assessment of tropically weathered and fractured gneissic aquifers using combined georesistivity and geostatistical methods, Journal of the Nigerian Society of Physical Sciences (2022) 497.
[47] P.E. Ndimele, A.O. Saba, I.O. Elegbede, T.L. Jolaosho, A.E. Ojewole, O.L. Eboh, M.O. Adigun, Source apportionment, ecological and health risk assessment of potentially toxic elements in water, sediment and blackchin Tilapia {Sarotherodon melanotheron (rüppell 1852)} from Lagos and Ologe lagoons, Lagos state, Nigeria, Journal of Trace Elements and Minerals (2024) 100173.
[48] M. Dey, A. Akter, S. Islam, S.C. Dey, T.R. Choudhury, K.J. Fatema, B.A. Begum, Assessment of contamination level, pollution risk and source apportionment of heavy metals in the Halda River water, Bangladesh, Heliyon 7 (12) (2021) 100173.
[49] B.U. Ukah, J.C. Egbueri, C.O. Unigwe, O.E. Ubido, Extent of heavy metals pollution and health risk assessment of groundwater in a densely populated industrial area, Lagos, Nigeria, International Journal of Energy and Water Resources 3 (4) (2019) 291–303.
[50] H. Rajkumar, P.K. Naik, M.S. Rishi, A new indexing approach for evaluating heavy metal contamination in groundwater, Chemosphere 245 (2020) 125598.
[51] J.C. Egbueri, C.O. Unigwe, Understanding the extent of heavy metal pollution in drinking water supplies from Umunya, Nigeria: an indexical and statistical assessment, Anal. Lett. 53 (13) (2020) 2122–2144.
[52] S. Saha, A.H.M. Reza, M.K. Roy, Hydrochemical evaluation of groundwater quality of the Tista floodplain, Rangpur, Bangladesh, Appl. Water Sci. 9 (8) (2019) 1–12.
[53] M. Hossain, P.K. Patra, Water pollution index–A new integrated approach to rank water quality, Ecol. Indicat. 117 (2020) 106668.
[54] H. El Fadili, M.B. Ali, M. El Mahi, A.T. Cooray, A comprehensive health risk assessment and groundwater quality for irrigation and drinking purposes around municipal solid waste sanitary landfill: a case study in Morocco, Environ. Nanotechnol. Monit. Manag. 18 (2022) 100698.
[55] H.M. Zakir, S. Sharmin, A. Akter, M.S. Rahman, Assessment of health risk of heavy metals and water quality indices for irrigation and drinking suitability of waters: a case study of Jamalpur Sadar area, Bangladesh, Environmental advances 2 (2020) 100005.
[56] S. Madhav, A. Ahamad, A. Kumar, J. Kushawaha, P. Singh, P.K. Mishra, Geochemical assessment of groundwater quality for its suitability for drinking and irrigation purpose in rural areas of Sant Ravidas Nagar (Bhadohi), Uttar Pradesh, Geology, Ecology, and Landscapes 2 (2) (2018) 127–136.
[57] L.A. Richards (Ed.), Diagnosis and Improvement of Saline and Alkali Soils (No. 60), US Government Printing Office, 1954.
[58] L.D. Doneen, The influence of crop and soil on percolating water, in: Proc. 1961 Biennial Conference on Groundwater Recharge, 1962, June, pp. 156–163.
[59] L. Wilcox, Classification and Use of Irrigation Waters, No. 969, US Department of Agriculture, 1955.
[60] I. Szabolcs, K. Darab, Radioactive Technique for Examining the Improving Effect of CaCO3 on Alkali (Szik) Soils, 1964.
[61] P. Balamurugan, P.S. Kumar, K. Shankar, Dataset on the suitability of groundwater for drinking and irrigation purposes in the Sarabanga River region, Tamil Nadu, India, Data Brief 29 (2020) 105255.
[62] United States Environmental Protection Agency, USEPA, Risk Assessment Guidance for Superfund. Volume 1: Human Health Evaluation Manual (Part E, Supplemental Guidance for Dermal Risk Assessment), Office of Superfund Remediation and Technology Innovation, Washington, DC, USA, 2004. EPA/540/R/99/005.
[63] J.C. Egbueri, C.N. Mgbenu, Chemometric analysis for pollution source identification and human health risk assessment of water resources in Ojoto Province, southeast Nigeria, Appl. Water Sci. 10 (4) (2020) 1–18.
[64] International Agency for Research on Cancer, Chemical agents and related occupations, IARC Monogr. Eval. Carcinog. Risks Hum. 100 (2012) 94.
[65] A.A. Oni, S.O. Babalola, A.D. Adeleye, T.E. Olagunju, I.A. Amama, E.O. Omole, O.G. Ohore, Non–carcinogenic and carcinogenic health risks associated with heavy metals and polycyclic aromatic hydrocarbons in well–water samples from an automobile junk market in Ibadan, SW–Nigeria, Heliyon 8 (9) (2022) 100173.
[66] C.P. Morice, J.J. Kennedy, N.A. Rayner, P.D. Jones, Quantifying uncertainties in global and regional temperature change using an ensemble of observational estimates: the HadCRUT4 data set, J. Geophys. Res. Atmos. 117 (D8) (2012).
[67] E.D. Sunkari, M. Abu, M.S. Zango, A.M.L. Wani, Hydrogeochemical characterization and assessment of groundwater quality in the kwahu–bombouaka group of the voltaian supergroup, Ghana, J. Afr. Earth Sci. 169 (2020) 103899.
[68] J.C. Egbueri, J.C. Agbasi, Combining data–intelligent algorithms for the assessment and predictive modeling of groundwater resources quality in parts of southeastern Nigeria, Environ. Sci. Pollut. Control Ser. 29 (38) (2022) 57147–57171.
[69] N.N. Odu, A.L. Omunakwe, M. Millicent, Comparative Assessment on the Physicochemical Water Quality of Wells and Boreholes in Two Rivers State Communities, 2020 (Nigeria).
[70] M.O. Onwuka, U.M.P. Amadi, Borehole design against saltwater intrusion in the coastal areas of Lagos State, Nigeria, in: Proceedings of the NIWASA Symposium, Port Harcourt, 1987, October, pp. 19–21.
[71] W.H.O. World Health Organization, Guidelines for Drinking-Water Quality: Fourth Edition Incorporating the First Addendum, WHO, Geneva, 2017.
[72] N.H. Hussin, I. Yusoff, W.Z. Wan Muhd Tahir, I. Mohamed, A.I.N. Ibrahim, A. Rambli, Multivariate statistical analysis for identifying water quality and hydrogeochemical evolution of shallow groundwater in Quaternary deposits in the Lower Kelantan River Basin, Malaysian Peninsula, Environ. Earth Sci. 75 (2016) 1–16.
[73] I. Rosborg, F. Kozisek, Drinking Water Minerals and Mineral Balance, Springer International Pu, 2016.
[74] US EPA (US Environmental Protection Agency), Risk–Based Concentration Table, United States Environmental Protection Agency, 2010. Available at: http://www.epa.gov/reg3hwmd/risk/human/index.htm.
[75] World Health Organization, WHO Global Water, Sanitation and Hygiene: Annual Report 2020, 2022.
[76] NSDQW, Nigerian standard for drinking water quality, Nigerian Industrial Standard NIS 554 (2007) 30. Standard Organization of Nigeria.
[77] C.L. Brierley, Bioremediation of metal-contaminated surface and ground waters, Geomicrobiol. J. 8 (3–4) (1990) 201–223.
[78] T.H.Y. Tebbutt, Principles of Water Quality Control, Elsevier, 2013.

[79] S. Dey, S. Singh, N.J. Raju, R.K. Mall, Hydrogeochemical characterization for groundwater quality and risk assessment in part of central Gangetic alluvium, India, Groundwater for Sustainable Development 25 (2024) 101108.
[80] A. Bouderbala, B.Y. Gharbi, Hydrogeochemical characterization and groundwater quality assessment in the intensive agricultural zone of the Upper Cheliff plain, Algeria, Environ. Earth Sci. 76 (2017) 1–17.
[81] D. Walker, N. Jovanovic, R. Bugan, T. Abiye, D. Du Preez, G. Parkin, J. Gowing, Alluvial aquifer characterisation and resource assessment of the Molototsi sand river, Limpopo, South Africa, J. Hydrol.: Reg. Stud. 19 (2018) 177–192.
[82] M.S. Zango, E.D. Sunkari, M. Abu, A. Lermi, Hydrogeochemical controls and human health risk assessment of groundwater fluoride and boron in the semi-arid North East region of Ghana, J. Geochem. Explor. 207 (2019) 106363.
[83] R. Yuan, Z. Li, S. Guo, Health risks of shallow groundwater in the five basins of Shanxi, China: geographical, geological and human activity roles, Environmental Pollution 316 (2023) 120524.
[84] Y. Zhou, P. Li, L. Xue, Z. Dong, D. Li, Solute geochemistry and groundwater quality for drinking and irrigation purposes: a case study in Xinle City, North China, Geochemistry 80 (4) (2020) 125609.
[85] Y. Mtoni, I.C. Mjemah, C. Bakundukize, M. Van Camp, K. Martens, K. Walraevens, Saltwater intrusion and nitrate pollution in the coastal aquifer of Dar es Salaam, Tanzania, Environ. Earth Sci. 70 (2013) 1091–1111.
[86] G. Cortecci, E. Dinelli, A. Bencini, A. Adorni-Braccesi, G. La Ruffa, Natural and anthropogenic SO4 sources in the Arno river catchment, northern Tuscany, Italy: a chemical and isotopic reconnaissance, Appl. Geochem. 17 (2) (2002) 79–92.
[87] E. Craswell, Fertilizers and nitrate pollution of surface and ground water: an increasingly pervasive global problem, SN Appl. Sci. 3 (4) (2021) 518.
[88] M. Schiavo, N. Colombani, M. Mastrocicco, Modeling stochastic saline groundwater occurrence in coastal aquifers, Water Res. 235 (2023) 119885.
[89] S. Najib, A. Fadili, K. Mehdi, J. Riss, A. Makan, Contribution of hydrochemical and geoelectrical approaches to investigate salinization process and seawater intrusion in the coastal aquifers of Chaouia, Morocco, J. Contam. Hydrol. 198 (2017) 24–36.
[90] S. Dey, N.J. Raju, W. Gossel, R.K. Mall, Hydrogeochemical characterization and geochemical modeling for the evaluation of groundwater quality and health risk assessment in the Varuna River basin, India, Environ. Geochem. Health (2023) 1–24.
[91] J. Mallick, C.K. Singh, M.K. AlMesfer, A. Kumar, R.A. Khan, S. Islam, A. Rahman, Hydro–geochemical assessment of groundwater quality in Aseer Region, Saudi Arabia, Water 10 (12) (2018) 1847.
[92] X. Li, J. Xiao, N. Chai, Z. Jin, Controlling mechanism and water quality assessment of arsenic in China's Yellow River Basin, J. Clean. Prod. 418 (2023) 137953.
[93] N. Chai, Z. Zhao, X. Li, J. Xiao, Z. Jin, Chemical weathering processes in the Chinese loess plateau, Geosci. Front. 15 (5) (2024) 101842.
[94] L. Ligavha–Mbelengwa, M. Gomo, Investigation of factors influencing groundwater quality in a typical Karoo aquifer in Beaufort West town of South Africa, Environ. Earth Sci. 79 (2020) 1–15.
[95] J. Chen, Q. Huang, Y. Lin, Y. Fang, H. Qian, R. Liu, H. Ma, Hydrogeochemical characteristics and quality assessment of groundwater in an irrigated region, Northwest China, Water 11 (1) (2019) 96.
[96] J. Liu, Y. Peng, C. Li, Z. Gao, S. Chen, An investigation into the hydrochemistry, quality and risk to human health of groundwater in the central region of Shandong Province, North China, J. Clean. Prod. 282 (2021) 125416, https://doi.org/10.1016/j.jclepro.2020.125416.
[97] R.J. Gibbs, Mechanisms controlling world water chemistry, Science 170 (3962) (1970) 1088–1090.
[98] M. Argamasilla, J.A. Barberá, B. Andreo, Factors controlling groundwater salinization and hydrogeochemical processes in coastal aquifers from southern Spain, Sci. Total Environ. 580 (2017) 50–68.
[99] P.J. Edwards, K.W. Williard, J.E. Schoonover, Fundamentals of watershed hydrology, Journal of contemporary water research & education 154 (1) (2015) 3–20.
[100] F. Martini, L. Fregna, M. Bosia, G. Perrozzi, R. Cavallaro, Substance–related disorders, in: Fundamentals of Psychiatry for Health Care Professionals, Springer International Publishing, Cham, 2022, pp. 263–295.
[101] S. Prasad, K.K. Yadav, S. Kumar, N. Gupta, M.M. Cabral–Pinto, S. Rezania, J. Alam, Chromium contamination and effect on environmental health and its remediation: a sustainable approaches, J. Environ. Manag. 285 (2021) 112174.
[102] O.C. Chika, E.A. Prince, Comparative assessment of trace and heavy metals in available drinking water from different sources in the centre of Lagos and off town (Ikorodu LGA) of Lagos State, Nigeria, Advanced Journal of Chemistry 3 (1) (2020) 94–104.
[103] P.N. Obasi, B.B. Akudinobi, Potential health risk and levels of heavy metals in water resources of lead–zinc mining communities of Abakaliki, southeast Nigeria, Appl. Water Sci. 10 (7) (2020) 1–23.
[104] I. Udousoro, S.I. Austin, Levels of some selected heavy metals in groundwater in Ebubu community, Eleme, Rivers state, Nigeria, Journal of Earth and Environmental Science Research 1 (2) (2019) 1–5.
[105] J.M. Gibson, A. Desclos, J. Harrington, S.P. McElmurry, R. Mulhern, Effect of community water service on lead in drinking water in an environmental justice community, Environmental Science & Technology 58 (3) (2024) 1441–1451.
[106] N. Singh, A. Kumar, V.K. Gupta, B. Sharma, Biochemical and molecular bases of lead–induced toxicity in mammalian systems and possible mitigations, Chem. Res. Toxicol. 31 (10) (2018) 1009–1021.
[107] M.A. Assi, M.N.M. Hezmee, M.Y.M. Sabri, M.A. Rajion, The detrimental effects of lead on human and animal health, Vet. World 9 (6) (2016) 660.
[108] M.A. Kamaruddin, M.S. Yusoff, L.M. Rui, A.M. Isa, M.H. Zawawi, R. Alrozi, An overview of municipal solid waste management and landfill leachate treatment: Malaysia and Asian perspectives, Environ. Sci. Pollut. Control Ser. 24 (2017) 26988–27020.
[109] F.S. Al–Fartusie, S.N. Mohssan, Essential trace elements and their vital roles in human body, Indian J. Adv. Chem. Sci. 5 (3) (2017) 127–136.
[110] T.O. Kolawole, C.A. Oyelami, J.O. Olajide-Kayode, M.T. Jimoh, K.W. Fomba, A.J. Anifowose, S.B. Akinde, Contamination and risk surveillance of potentially toxic elements in different land-use urban soils of Osogbo, Southwestern Nigeria, Environ. Geochem. Health 45 (7) (2023) 4603–4629.
[111] A.F. Bon, T.A.M.N. Ngoss, G.E. Mboudou, L.A. Banakeng, J.R.N. Ngoupayou, G.E. Ekodeck, Groundwater flow patterns, hydrogeochemistry and metals background levels of shallow hard rock aquifer in a humid tropical urban area in sub-Saharan Africa-A case study from Olézoa watershed (Yaoundé-Cameroon), J. Hydrol.: Reg. Stud. 37 (2021) 100904.
[112] K.O. Ibrahim, M. Gomo, S.A. Oke, Groundwater quality assessment of shallow aquifer hand dug wells in rural localities of Ilorin northcentral Nigeria: implications for domestic and irrigation uses, Groundwater for Sustainable Development 9 (2019) 100226.
[113] P.B. McMahon, K. Belitz, J.E. Reddy, T.D. Johnson, Elevated manganese concentrations in United States groundwater, role of land surface–soil–aquifer connections, Environ. Sci. Technol. 53 (1) (2018) 29–38.
[114] V. Kumar, S.K. Dwivedi, A review on accessible techniques for removal of hexavalent Chromium and divalent Nickel from industrial wastewater: recent research and future outlook, J. Clean. Prod. 295 (2021) 126229.
[115] R.J. Reeder, M.A. Schoonen, A. Lanzirotti, Metal speciation and its role in bioaccessibility and bioavailability, Rev. Mineral. Geochem. 64 (1) (2006) 59–113.
[116] H. Kumar, G. Singh, V.K. Mishra, R.P. Singh, P. Singh, Airborne heavy metals deposition and contamination to water resources, in: Metals in Water, Elsevier, 2023, pp. 155–173.
[117] F. Stagnari, S. Jan, G. Angelica, P. Michele, Sustainable agricultural practices for water quality protection, Water stress and crop plants: a sustainable approach 1 (2016) 75–85.
[118] J.B. Kowalska, R. Mazurek, M. Gąsiorek, T. Zaleski, Pollution indices as useful tools for the comprehensive evaluation of the degree of soil contamination–A review, Environ. Geochem. Health 40 (2018) 2395–2420.
[119] I. Stavi, N. Thevs, S. Priori, Soil salinity and sodicity in drylands: a review of causes, effects, monitoring, and restoration measures, Front. Environ. Sci. 9 (2021) 712831.
[120] C.P. Ahada, S. Suthar, Assessing groundwater hydrochemistry of Malwa Punjab, India, Arabian J. Geosci. 11 (2018) 1–15.
[121] S.U. Wali, M.A. Gada, K.J. Umar, A. Abba, A. Umar, Understanding the causes, effects, and remediation of salinity in irrigated fields: a review, International Journal of Agriculture and Animal Production (IJAAP) ISSN (2021) 2799, 0907.

[122] S.M. Saghebian, M.T. Sattari, R. Mirabbasi, M. Pal, Ground water quality classification by decision tree method in Ardebil region, Iran, Arabian J. Geosci. 7 (2014) 4767–4777.
[123] M. Hossain, P.K. Patra, S.N. Begum, C.H. Rahaman, Spatial and sensitivity analysis of integrated groundwater quality index towards irrigational suitability investigation, Appl. Geochem. 123 (2020) 104782.
[124] S.K. Srivastava, Assessment of groundwater quality for the suitability of irrigation and its impacts on crop yields in the Guna district, India, Agric. Water Manag. 216 (2019) 224–241.
[125] L. Rahimi, H. Amanipoor, S. Battaleb–Looie, Effect of salinity of irrigation water on soil properties (abadan plain, SW Iran), Geocarto Int. 36 (16) (2021) 1884–1903.
[126] R. Pivić, J. Maksimović, Z. Dinić, D. Jaramaz, H. Majstorović, D. Vidojević, A. Stanojković–Sebić, Hydrochemical assessment of water used for agricultural soil irrigation in the water area of the three Morava Rivers in the Republic of Serbia, Agronomy 12 (5) (2022) 1177.
[127] X. Ke, S. Gui, H. Huang, H. Zhang, C. Wang, W. Guo, Ecological risk assessment and source identification for heavy metals in surface sediment from the Liaohe River protected area, China, Chemosphere 175 (2017) 473–481.
[128] D. Karunanidhi, P. Aravinthasamy, M. Deepali, T. Subramani, E.D. Sunkari, Appraisal of subsurface hydrogeochemical processes in a geologically heterogeneous semi–arid region of south India based on mass transfer and fuzzy comprehensive modeling, Environ. Geochem. Health 43 (2021) 1009–1028.
[129] S. Kükrer, S. Şeker, Z.T. Abacı, B. Kutlu, Ecological risk assessment of heavy metals in surface sediments of northern littoral zone of Lake Çıldır, Ardahan, Turkey, Environ. Monit. Assess. 186 (2014) 3847–3857.
[130] H.F. Kaiser, An index of factorial simplicity, Psychometrika 39 (1) (1974) 31–36.
[131] H. Cüce, E. Kalipci, F. Ustaoğlu, M.A. Dereli, A. Türkmen, Integrated spatial distribution and multivariate statistical analysis for assessment of ecotoxicological and health risks of sediment metal contamination, Ömerli Dam (Istanbul, Turkey), Water, Air, Soil Pollut. 233 (6) (2022) 199.
[132] P. Cerchier, L. Pezzato, C. Gennari, E. Moschin, I. Moro, M. Dabalà, PEO coating containing copper: a promising anticorrosive and antifouling coating for seawater application of AA 7075, Surf. Coating. Technol. 393 (2020) 125774.
[133] J. Wieczorek, A. Baran, Pollution indices and biotests as useful tools for the evaluation of the degree of soil contamination by trace elements, J. Soils Sediments (2022) 1–18.
[134] D. Khadija, A. Hicham, A. Rida, E. Hicham, N. Nordine, F. Najlaa, Surface water quality assessment in the semi–arid area by a combination of heavy metal pollution indices and statistical approaches for sustainable management, Environmental Challenges 5 (2021) 100230.
[135] S. Tong, H. Li, M. Tudi, X. Yuan, L. Yang, Comparison of characteristics, water quality and health risk assessment of trace elements in surface water and groundwater in China, Ecotoxicol. Environ. Saf. 219 (2021) 112283.
[136] Y. Liu, R. Ma, Human health risk assessment of heavy metals in groundwater in the luan river catchment within the north China Plain, Geofluids 2020 (1) (2020) 8391793.
[137] L. Zhu, M. Yang, X. Chen, J. Liu, Health risk assessment and risk control: drinking groundwater in Yinchuan Plain, China, Exposure and Health 11 (1) (2019) 59–72.
[138] M. Feki–Tounsi, A. Hamza–Chaffai, Cadmium as a possible cause of bladder cancer: a review of accumulated evidence, Environ. Sci. Pollut. Control Ser. 21 (2014) 10561–10573.
[139] S. Liu, M. Costa, Carcinogenicity of metal compounds, in: Handbook on the Toxicology of Metals, Academic Press, 2022, pp. 507–542.